Ethiopian rift shoulders, where the highest values are related to the flexural uplift (Weissel et al., 1995; Sembroni et al., 2016a; Stüwe et al., 2022; Fig. S2), and the Ethiopian Plateau, because of the strong fluvial incision (Sembroni et al., 2016b, 2021; Fig. S2). The elastic thickness values obtained (Table S1) together with published seismic tomography data (Priestley et al., 2008; Chang and Van der Lee, 2011; Hansen et al., 2012; Chen et al., 2015) well correlate with the topographic pattern of the region and point to a mantle supported uplift (Chen et al., 2015). The feedback between erosion and seafloor spreading in the Red Sea area (Stüwe et al., 2022) could have enhanced the flexural uplift at the Red Sea margins inhibiting the capture of the swell top surface by rivers draining the inner part of the Red Sea shoulders. Portions of this surface has been locally studied in the past (Coltorti et al., 2007; Gani et al., 2007; Avni et al., 2012; Bar et al., 2016; Sembroni et al., 2016a, 2016b; Sembroni and Molin, 2018; Sembroni et al., 2021), but the topographic analysis performed here allows designating different fragments. They are located roughly along the axis of the swell ridge at an elevation between 800 m, in the north, and 2700 m, in the south (Fig. S1). The overall elevation pattern and geometry of the surface resembles the filtered, residual, and dynamic topographies (Figs. 7a, b and 10b, f). In turn, the filtered topography at 200 km approximates the present topography except for the Red Sea margins where the flexural component is dominant (Figs. 8 and 9). This suggests that the swell top surface and part of the present topography of the study area can be related to mantle processes (Sengör, 2001; Daradich et al., 2003; Forte et al., 2010; Moucha and Forte, 2011; Faccenna et al., 2013).

Recent studies on the uplift history of the Ethiopian-Somalian and Yemen plateaux (Sembroni et al., 2016a; Faccenna et al., 2019; Sembroni et al., 2021) and the Jordan plateau (Bar et al., 2016) show that the southern portion of the swell (Horn of Africa) in the lower Oligocene was at elevations very close to those currently shown by the swell top surface, while the northern one (Levant region) reached the elevation of ~1000 m (the average elevation of the swell top surface in this region) at the end of upper Miocene (Fig. 16). This means that the bulk of the uplift in most of the study area occurred between the Oligocene and Miocene and that the present topography is very similar to the one reached in that period, partly modified by surface erosion, flood basalt emplacement, and flexural uplift along the Red Sea and MER margins. This is also confirmed by thermochronology data showing a rapid and significant exhumation phase during that period (Boone et al., 2021; Lanari et al., 2023) with rates between 0.1 and 0.3 mm/yr in the northern portion of the Red Sea (Lanari et al., 2023).

The opening of the Red Sea begun in its southernmost portion between the end of the Oligocene and the beginning of the Miocene (Boone et al., 2021, and references therein). This would relate, at least temporally, this event to the deep process underlying the formation of the swell but does not allow to define with certainty whether the same process also caused the opening of the Red Sea. Several studies (McQuarrie et al., 2003; Bellahsen et al., 2003; Bosworth et al., 2005; Koptev et al., 2018; Khalil et al., 2020) agree that the Red Sea and the Gulf of Aden rifts were mainly driven by slab pull occurred along the Bitlis-Zagros subduction front, with plume-related magmatism acting to generate extension in the Afar and Red Sea.

However, the thermo-mechanical weakening of the lithosphere related to plume impingement together with pre-existing lithospheric heterogeneities seem to have played a role in rift evolution (e.g., Koptev

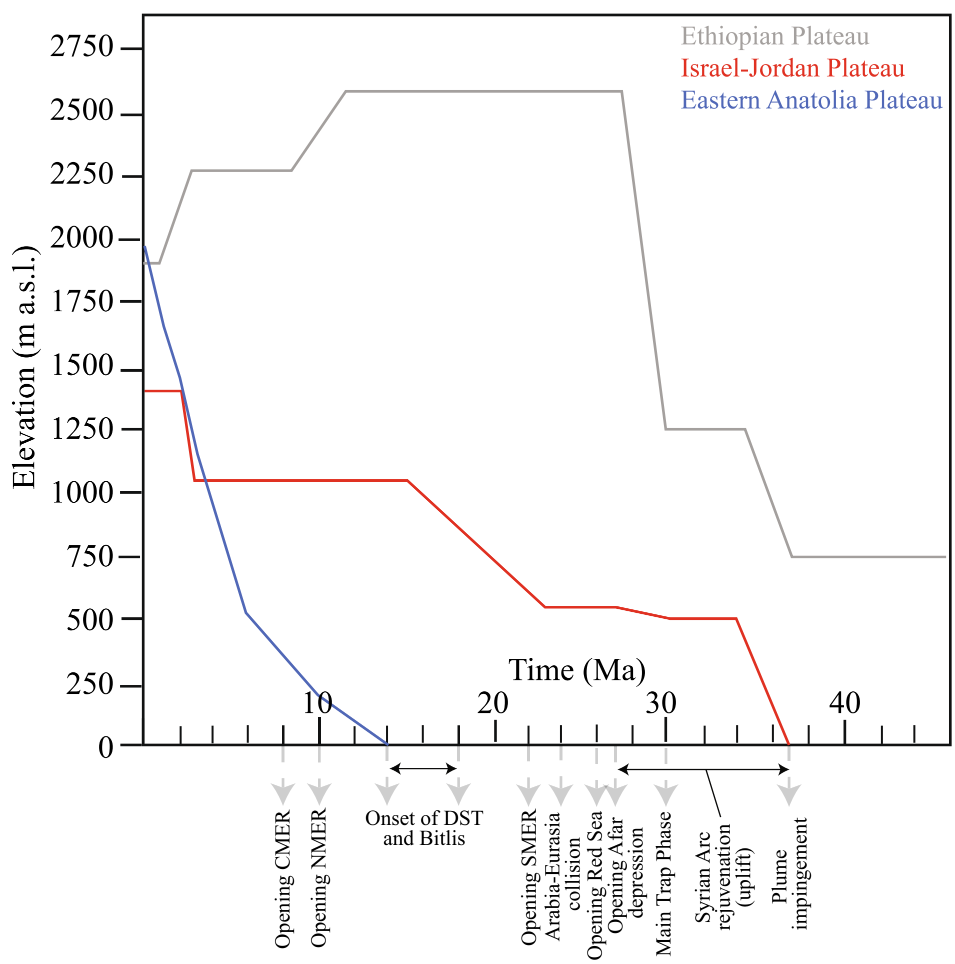

Fig. 16. Uplift histories of the Ethiopian, Jordan, and Eastern Anatolian plateaux according to recent studies (respectively Faccenna et al., 2019; Bar et al., 2016; Molin et al., 2023).

et al., 2018; Khalil et al., 2020). The analysis of flexural uplift along the Red Sea margins confirms the progressive northwards opening of the rift with an uplift increasing from north to south (Fig. 9a and Table S1). The greatest elevations (w_0) and wavelength (α) were found on the Arabian plate. Despite the high values (see Table S1), the flexural uplift marginally influenced the topographic configuration of the EAAS since its effect becomes close to zero at a maximum distance of ~250 km from the Red Sea margins (Fig. 9a). The same analysis performed in the Main Ethiopian Rift area suggests again a southward increase in flexural uplift (from 500 to 1200 m) with maximum wavelength of ~200 km from the rift shoulders (Weissel et al., 1995; Sembroni et al., 2016a).

The comparison between flexural uplift data and filtered topographies in the Red Sea region (Fig. 9b) clearly shows how the topography in this area is the result of the interaction between shallower (flexural uplift) and deeper (mantle plume) processes. Indeed, the topographic profile across the Red Sea presents neither a pattern typical of a rift margin subjected to flexural unloading (green curve in Fig. 9b) nor that of an area characterized by bulging due to rising hot mantle material (blue curve in Fig. 9b) but something in between: for the first 200 km the green curve is what best approximates the topography; beyond that distance the profile follows the blue curve.

Like topography and flexural uplift, the areal distribution of volcanism shows a marked asymmetry as much in the Horn of Africa as in the Arabian Peninsula (Fig. 14). Our analysis reveals that in the Horn of Africa most of the volcanic deposits outcrop to the west of the Main Ethiopian Rift (cf. Sembroni et al., 2016a). Conversely, in the Arabian Peninsula, most of volcanic fields follows the axis of the EAAS to the E of the Red Sea (Fig. 14). Along the strike of this axis, from Ethiopia to Turkey, there is an overall decrease in the age of volcanics and a parallel decrease in topography (Fig. 15c). This implies that a single main mantle upwelling is sufficient to explain the present topographic configuration and the chronology of volcanic deposits, as seismic tomography and geochemical data seem to confirm (Priestley et al., 2008; Hansen et al., 2012; Faccenna et al., 2013; Schaeffer and Lebedev, 2013; Auer et al., 2014; Gvirtzman et al., 2016; Lu et al., 2019; Thrastarson et al., 2024). If, as claimed in some studies (e.g., Chang and Van der Lee, 2011; Koulakov et al., 2016; Chang et al., 2020), there were more sources of volcanism (more arrivals of hot mantle material) or there was a different path, both the topography and volcanics age distribution would likely show a more irregular pattern. However, the concomitance of other local processes underlying Arabian volcanism cannot be ruled out. For example, the recent volcanism (< 12 Ma) in southwestern Arabia has been speculated to be related to decompression melting in the mantle lithosphere caused by flexural uplift (Stüwe et al., 2022).

The appearance of magmatism below the Arabian Peninsula seems to be spread over a very large area. This would imply the presence of a very low-viscosity asthenosphere as seems to be confirmed by seismic, petrological, and geochemical data (Hua et al., 2023).

The ages of the volcanic deposits are progressively younger toward the north, some of which may be due to younger deposits partly or completely covering older ones. Despite this limitation, the frequency of volcanic deposits ages shows a bimodal trend with a brief period (few millions of years) of partial quiescence characterized by few events (Fig. 15a, b). On the Arabian plate, the areal distribution of volcanics before and after this time span shows a marked change. In particular, the old volcanics were emplaced along NW-SE dikes inherited from Precambrian tectonic lineaments (Najd Fault System; Johnson et al., 2017 and references therein). Conversely, the new volcanic centers are aligned N-S (Fig. 14). The age of the partial quiescence shifts to younger ages from south (16–18 Ma) to north (8–10 Ma; Fig. 15a, b). The older quiescence period is coincident with the advanced stage of the Arabia-Eurasia collision at the Bitlis collision zone (18–14 Ma – Okay et al., 2010; Ballato et al., 2011; Cavazza et al., 2018, 2019; Gusmeo et al., 2021; Darin and Umhoefer, 2022) and the activation of the Dead Sea transform fault (17–20 Ma – Quennell, 1958; Freund et al., 1970; Garfunkel, 1981; Garfunkel et al., 1981; Joffe and Garfunkel, 1987; Bosworth et al., 2005; Nuriel et al., 2017). These processes caused the counterclockwise rotation of the Arabian plate and the change in the direction of maximum compression (at the Bitlis-Zagros front) and extension (in the Red Sea and Gulf of Aden) from NE-SW to N-S (Boone et al., 2021, and references therein). This may have caused the closure of the NW-SE Precambrian lineaments and the opening of new N-S lineaments as was already proposed in the case of the Harrat Ash Shaam in Syria (Al Kwatli et al., 2012).

The pause and renewal of volcanism in the study area are followed, respectively, by increases and decreases in the number of mammal evolution lineages (de Vries et al., 2021). Although de Vries et al. (2021) cite also the climate factor as a contributing cause, the close correlation between volcanism pauses and renewal and the mammal evolution lineages trend, makes the geological factor predominant as already demonstrated in other parts of the world (e.g., Deccan and Siberia; Prave et al., 2016; Ernst and Youbi, 2017).

In summary, the present topography of the region spanning from Ethiopia to Syria shows an elongated ridge with a roughly NNW-SSE direction. It originates in Ethiopia, where it presents the greatest elevations and amplitude, and extends mainly into the Arabian plate with decreasing elevation and amplitude toward the north. The ridge is well described by the Oligocene low-relief surfaces and by the trend of filtered (200 and 400 km), residual, and dynamic topographies (Figs. 7, 10, 11). The same area has lower lithospheric thickness and higher residual and dynamic topographies respect to the surroundings and has negative P- and S-wave velocity and gravity anomalies (Fig. 10; Benoit et al., 2006a, 2006b; Priestley et al., 2008; Chang and Van der Lee, 2011; Hansen et al., 2012; Schaeffer and Lebedev, 2013; Auer et al., 2014; Chen et al., 2015; Gvirtzman et al., 2016; Lu et al., 2019; Boyce et al., 2021, 2023; Ebinger et al., 2024; Thrastarson et al., 2024). The decrease of filtered topography from Ethiopia to Syria is very similar to the trend of the volcanic deposits age, decreasing from south to north. All these data indicate the presence of a main single process which sculpted the past and present topographic configuration of the area. This process, having a wavelength of >200 km, is likely subcrustal as it exceeds flexural wavelengths. As already stated in the previous works on the study area (Faccenna et al., 2013; Gvirtzman et al., 2016; Agostini et al., 2021; Hua et al., 2023) this deep seated process may be identified with the upwelling of the Afar Superplume below the Ethiopian lithosphere that, taking advantage of prior discontinuities and/or pression gradients, channeled to the Levant region in a few million years causing the tilting to the SE of the Arabian Peninsula discussed in several studies (Sengör, 2001; Daradich et al., 2003). The northward progression of plume induced flow as discussed by Faccenna et al. (2013) is also broadly consistent with time dependent mantle convection reconstructions for the region (e.g. Moucha and Forte, 2011; Faccenna et al., 2019; Straume et al., 2024).

According to geological data (Avni et al., 2012; Bar et al., 2016) the planation surface detected between the southern Levant area and the northern Red Sea region can be dated at the Oligocene. However, the region rose from 500 m to 1000 m elevation only at the end of upper Miocene (Bar et al., 2016; Fig. 16). This means that the arrival of the superplume in this sector may be placed at the beginning of the Miocene (Fig. 16). If this is correct, the tilting of Arabia can be placed between the impingement of the plume beneath Ethiopia (Late Eocene; Ebinger and Sleep, 1998; Sengör, 2001; Ebinger et al., 2024) and the arrival of the same plume in the Levant region (upper Miocene). This is confirmed by stratigraphic data which indicate a strong subaerial erosion phase throughout the Arabian Peninsula between the end of Paleogene and the beginning of the Neogene, immediately after a long transgression phase which established shallow marine condition over eastern Arabia since early Paleocene (Alsharhan and Nairn, 1995; Sengör, 2001; Ziegler, 2001). This phase generated an unconformity between the Paleocene and Miocene sediments and the shifting of the eastern Arabia coastline by >500 km to the northeast (Alsharhan and Nairn, 1995; Ziegler, 2001; Fig. 17). Looking at the coastline reconstruction of the eastern sector of

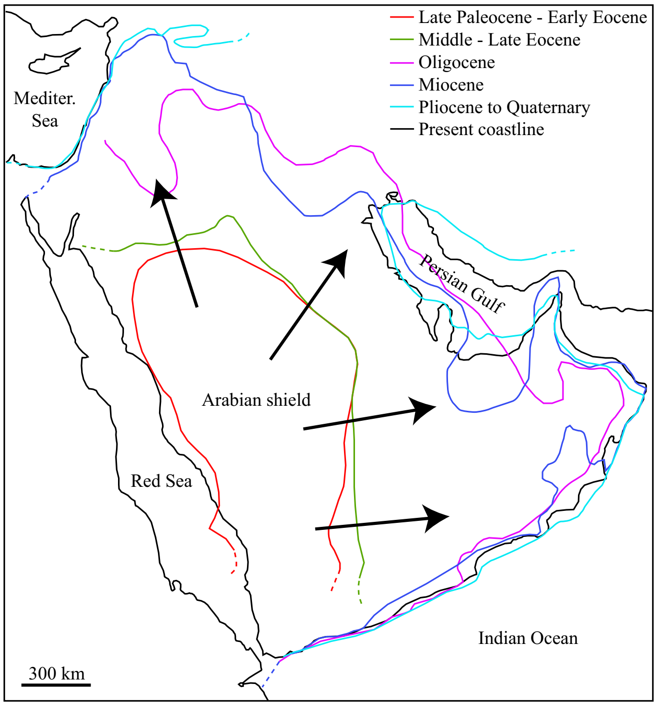

Fig. 17. Map showing the migration of the eastern Arabia coastline from Late Paleocene to Quaternary (modified after Alsharhan and Nairn, 1995 and Ziegler, 2001).

Arabia (Fig. 17), it is interesting to note that the northeastward shift appears to be parallel to the swell axis (Figs. 7, 8, 11). This suggests a direct involvement of the northward passage of the superplume in the coastline migration (cf. Straume et al., 2024). The presence of a new relief in the western side of Arabia is also confirmed by huge volumes of sands deposited from an easterly flowing river network between late Oligocene and early Miocene in an area comprising Saudi Arabia, Kuwait, and southeastern Iraq (Alsharhan and Nairn, 1995; Ziegler, 2001; Barrier and Vrielynck, 2008).

On the other hand, mantle flow took a longer time to reach Turkey. In fact, in the middle Miocene, the area was still under sea level (Molin et al., 2023 and references therein; Fig. 18). The uplift of Anatolia and in particular of the Eastern Anatolian Plateau is debated. Different models have been proposed: 1) mantle delamination (Göğüş and Pysklywec, 2008; Keskin, 2003; Bartol and Govers, 2014; Kounoudis et al., 2020); 2) slab break-off (Bottrill et al., 2012; Faccenna et al., 2006; Keskin, 2003; Schildgen et al., 2014); 3) mantle asthenosphere support (Faccenna et al., 2013; Keskin, 2007; Şengül Uluocak et al., 2021). Recently, Molin et al. (2023) tried to reconcile these three model in a single evolutionary scenario where at ~10–11 Ma the slab break-off drove the formation of a slab window which continued to widen until ~4–5 Ma (Faccenna et al., 2006, 2013; Schildgen et al., 2014). Such a corridor could have allowed the plume to reach the base of the Eastern Anatolian Plateau, as confirmed by the basaltic volcanism mainly Quaternary in age in that area (Figs. 14, 15a, c, 18). Recent upper mantle seismic tomographic models (e.g. Kounoudis et al. 2020), seismic anisotropy studies (e.g. Paul et al., 2014; Merry et al., 2021), and residual topography calculations (e.g. Ogden and Bastow, 2022) seem to confirm the requirement for a mantle contribution to plateau uplift (cf. Straume et al., 2024).

The path of mantle flow throughout the region deeply influenced also the evolution of the main river networks: the Nile and the Euphrates-Tigris drainage systems. Indeed, both river networks source from areas of positive residual and dynamic topographies and have their base level in regions characterized by negative values (Fig. 10). Geological (Garzanti et al., 2006; Padoan et al., 2011; Sembroni et al., 2016a), geophysical (Faccenna et al., 2019, and references therein), and thermochronological data (Pik et al., 2003) indicate that the Nile River establish a connection between the Ethiopian plateau and the Mediterranean since at least Oligocene sustained by the upwelling of the Afar superplume at its source (Faccenna et al., 2019). Similarly, the first appearance of the Euphrates River is dated back to the middle Eocene when the subduction started at the Bitlis front (Okay et al., 2010; Ballato et al., 2011; Cavazza et al., 2018, 2019; Gusmeo et al., 2021; Darin and Umhoefer, 2022) and the whole region passed from marine to continental conditions (Molin et al., 2023, and references therein). The successive evolution of the river with the progressive migration of the coastline to the southeast and the consequent lengthening of the river course could be related partly to the ongoing subduction and partly to the arrival of Afar superplume in the northern Arabia region at late Miocene (Molin et al., 2023).

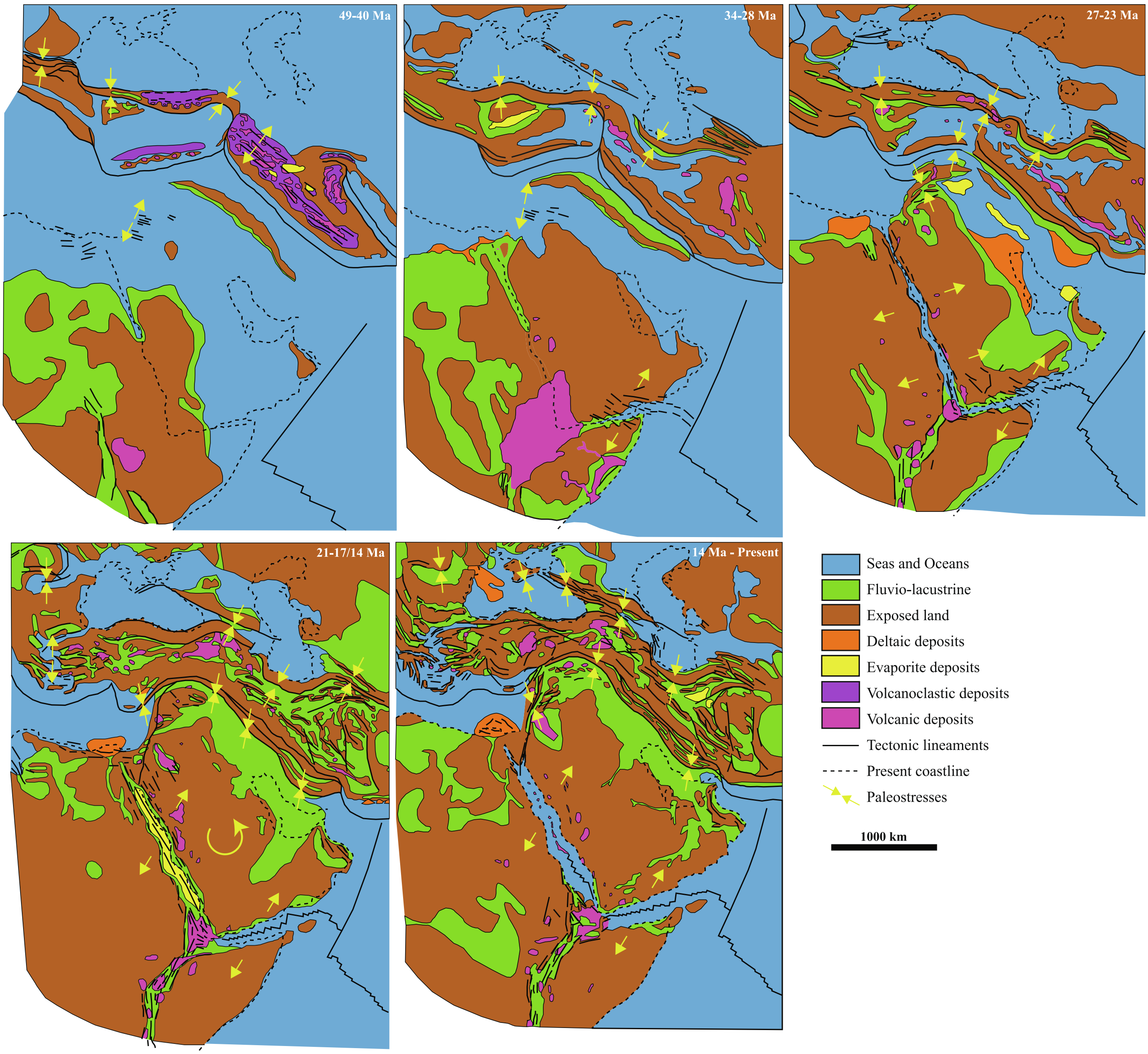

Fig. 18. Tectonic evolution of the study area (modified after Barrier and Vrielynck, 2008).

These data show how mantle processes can sculpt the surface of the Earth over tens of millions of years and support the idea expressed by Faccenna et al. (2019) that long-lived intra-continental rivers dynamics may provide indication of dynamic topography variations.

6.1. Tectonic evolution of the study area

The tectonic evolution of the study area can be summarized as follows (Figs. 18, 19):

45–35 Ma: Plume impingement occurred beneath Ethiopia, causing early uplift and volcanism mainly in southern Ethiopia.

31–29 Ma: Trap basalts are emplaced all over the Horn of Africa and the SW corner of the Arabian Peninsula forming an extended plateau. At about the same time (28–27 Ma) basalts poured out also in the western sector of Saudi Arabia from dikes and volcanoes aligned to Precambrian NW-SE structures. About 2/3 of the mammal fauna in the Afro-Arabia region becomes extinct (de Vries et al., 2021).

27–23 Ma: Volcanism continued in Arabia while a relative pause has been registered in Ethiopia highlands (formation of intratrappean levels; Abbate et al., 2014). Parallel to this pause in volcanism an increase in mammal fauna occurred in the region until about 20 Ma (de Vries et al., 2021). During this time the Oligocene planation surface formed in the Sinai and Levant areas (Avni et al., 2012). The uplift in the Oligocene formed almost all the topography of the Horn of Africa and the SW corner of the Arabian Peninsula. Meanwhile, the Gulf of Aden opened, and the Red Sea began to propagate from south to north (as well as the related flexural uplift as suggested by thermochronology data; Boone et al., 2021, and references therein). The tilting to the SE of the Arabia Peninsula began, testified by a strong erosion phase throughout Arabia and the northeastward shifting of the eastern Arabia coastline (Alsharhan and Nairn, 1995; Ziegler, 2001). An easterly flowing river network carried huge volume of sands eroded from the uplifted western Arabia to the Iraq-Persian Gulf area where a large deltaic system formed.

21–17/14 Ma: At the end of upper Miocene the Levant region experienced strong uplift which increased elevation from 500 to 1000 m (Bar et al., 2016; Fig. 16). Volcanic activity on the Ethiopian-Somalian

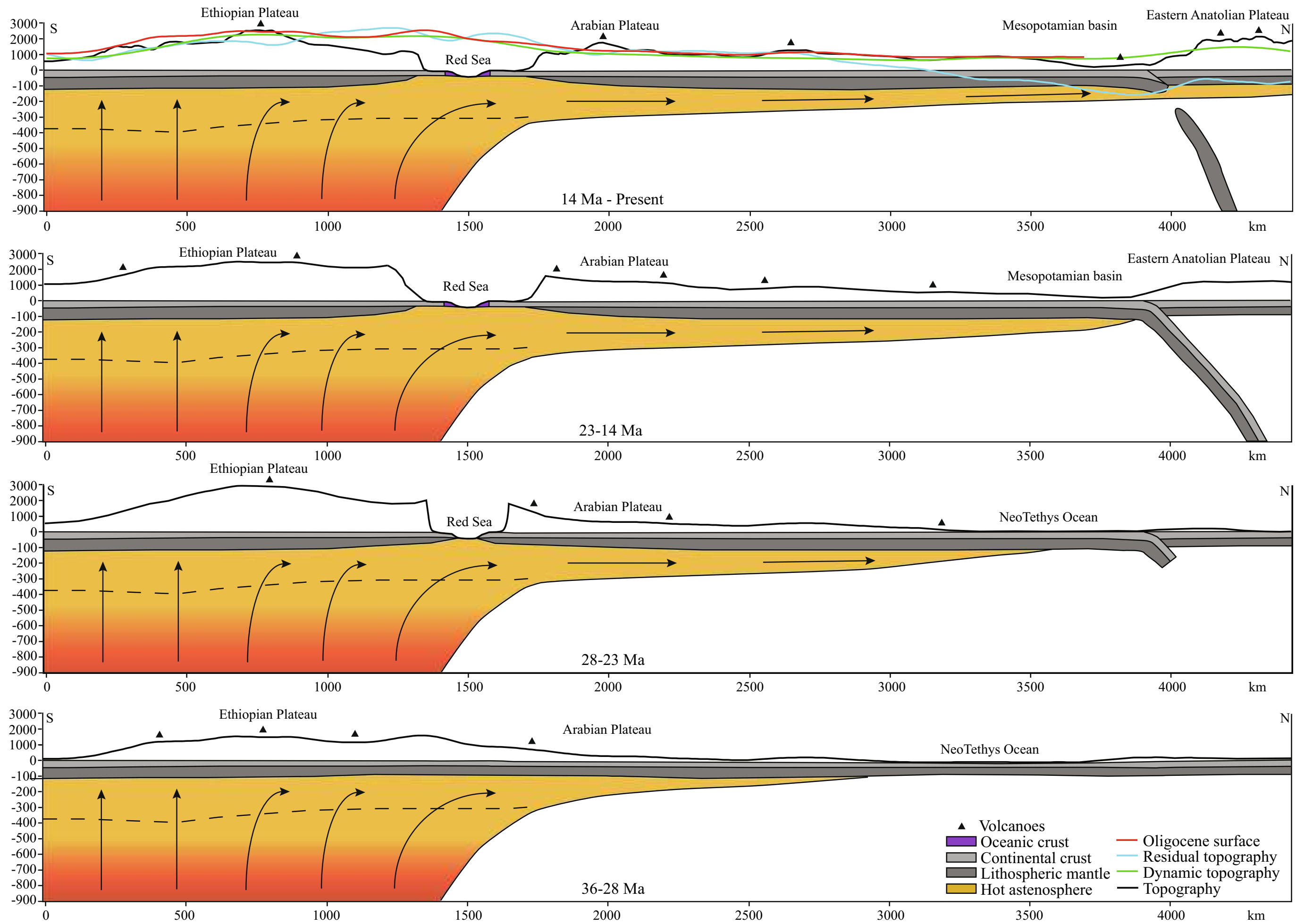

Fig. 19. Topographic evolution of the study area represented along a S—N trending topographic profile from Ethiopia to Eastern Anatolia. Note the lateral migration of the mantle flow and the parallel increase of surface topography (see text for further explanations).

plateau (shield volcanoes) and in the Ethiopian rift started over. In parallel, another dramatic decline in mammals occurred (de Vries et al., 2021). The stress regime changed: the Arabian plate rotates counterclockwise, and the direction of maximum compression becomes ~N-S. At the same time, the Dead Sea Transform Fault developed. A brief pause in volcanism in both Arabia and Horn of Africa occurred in coincidence with this change in the stress regime.

14 Ma-Present: Volcanism resumed in most of the study area. As a demonstration of the change in stress regime, the new volcanic edifices in Arabia are aligned ~N-S. It is at this stage that the most extensive volcanic fields formed in Arabia Peninsula. The eastern portion of Anatolia is strongly uplifted as demonstrated by geological data (passage from marine to continental deposition; Fig. 18), dating of Euphrates R. fluvial terraces (Demir et al., 2007) and river network analysis (Molin et al., 2023).

7. Conclusions

The East Africa - Arabia region has long been studied because of its anomalously high topography, volcanism, and active rifting. There is broad consensus about the role of mantle plumes in generating this high elevation, but the number of plumes and the uplift patterns are debated. We contribute to this discussion by providing an integrative evolutionary model of the region which seeks to integrate the range of constraints we have reviewed here. The main results are the following:

1. The EAA swell is a NNW-SSE trending ridge extending from Ethiopia to Jordan with amplitude and elevation gradually increasing from north (800 km and 800 m) to south (1600 km and 2700 m). Its continuity is interrupted to the south by the Turkana tectonic depression and to the north by the Mesopotamian foredeep basin whose depression may be related to the flexure of the lithosphere by subduction as confirmed by dynamic topography modeling. The area occupied by the swell presents thin lithosphere, high residual and dynamic topography, underlain by low seismic velocity anomalies.
2. The swell top is characterized by low relief surfaces, Oligocene in age, located roughly along the axis. The envelope of these surfaces represents the swell top surface which extends for >4000 km from Ethiopia to Jordan with present elevation decreasing from south (2500 m) to north (900 m).
3. The elevation pattern and geometry of the swell top surface resembles the filtered (200 and 400 km), residual, and dynamic topography, suggesting that the this surface is caused by mantle convective processes. Moreover, the uplift pattern of the southern portion of the swell show that the surface was at elevation close to the present one since the beginning of the lower Oligocene, while in the northern portion it reached ~1000 m at the end of the upper Miocene. Such a shift in uplift histories could match the migration pattern of the mantle plume, and indicates that most of the present topography is mainly the surface expression of mantle plume impingement.
4. The migration of mantle flow from eastern Africa drove the tilting of the Arabian Peninsula between late Eocene and upper Miocene.

Stratigraphic data indicate an erosion phase in the Arabian Peninsula between the end of Paleogene and the beginning of the Neogene and a significant shifting of the eastern Arabia coastline to the northeast which could constrain such an event.

5. The Nile and Euphrates-Tigris river networks source from areas of positive residual and dynamic topography and have their base level in regions characterized by negative values. This suggest that the formation and evolution of these drainage systems are influenced by mantle processes. In particular, the stable presence of a mantle upwelling beneath east Africa and the progressive migration of mantle flow to Turkey contributed to the formation of the Nile (Oligocene) and Euphrates-Tigris (Middle Miocene) river networks and to the maintenance of their path through tens of millions of years.
6. The incision pattern (local relief) on the top and on both flanks of the swell is low except for the rift margins, where the higher values are related to the flexural uplift, and of the Ethiopian Plateau because of the strong fluvial erosion.
7. Analysis of flexural uplift at the Red Sea margins shows an increase in uplift from south to north confirming thermochronological data from literature. In general, the western margin presents lower values than the eastern one, while the deformation related to flexural is visible up to ~250 km from the Red Sea margins. The comparison between flexural data and filtered topography confirms that the Red Sea region topography is the result of the interaction between shallower (flexural uplift) and deeper (mantle plume) processes.
8. The distribution of ages of volcanic deposits shows a gradual decrease in maximum age from Ethiopia to Turkey which broadly follows the curves of filtered topography extracted along the axis of the swell.
9. Along the swell axis volcanoes and basaltic lava fields are located. The frequency of volcanic deposits ages shows a bimodal trend with peaks separated by a brief period of low volcanic activity with a trend toward younger ages from south to north. In particular, the older quiescence period is coeval with the advanced stage of the Arabia-Eurasia collision at the Bitlis zone and the activation of the Dead Sea Transform Fault. These processes caused the counterclockwise rotation of the Arabian plate and the change in the direction of maximum compression from NE-SW to N-S favoring the opening of N-S trending tectonic lineaments and the closure of old NW-SE ones. In confirmation of this, Arabian volcanics older than 16 Ma emplaced through NW-SE-trending dikes, while younger deposits appear aligned in a N-S direction.

All these results point to the presence of a single process which shaped the past and present topographic configuration of the region, the upwelling of the Afar superplume. Once the plume reached the base of the lithosphere below the Horn of Africa, it flowed laterally toward the Levant area by exploiting pre-existing lithospheric structure, and then reached the Anatolian Plateau, facilitated by slab break-off and the consequent formation of a slab window. The buoyancy of the mantle material below the lithosphere generated the East African-Arabia swell interrupted to the north by the Mesopotamian foredeep basin.

Declaration of competing interest

Claudio Faccenna reports financial support was provided by Italian Research Ministry. If there are other authors, they declare that they have no known competing financial interests or personal relationships that could have appeared to influence the work reported in this paper.

Data availability

The original data supporting this research are available in the supplementary material or on request.

Acknowledgments

We thank the editor and anonymous reviewers for their efforts and comments which served to improve this manuscript from its original version. We also thank Alistair Boyce for sharing his Moho constraint compilation, as well as all authors for publishing SKS splitting and seismic tomography models openly. Several figures were generated with the Generic Mapping Tools by the late, great Pal Wessel (Wessel et al., 2019). This work has been supported by the project "Intraplate deformation, magmatism and topographic evolution of a diffuse collisional belt: Insights into the geodynamics of the Arabia-Eurasia collisional zones" funded by the Italian Research Ministry (MUR-PRIN 2017–2021). We thank all project participants for many fruitful discussions. TWB was supported by NSF EAR-1925939.

Appendix A. Supplementary data

Supplementary data to this article can be found online at https://doi.org/10.1016/j.earscirev.2024.104901.

References

Abbate, E., Bruni, P., Ferretti, M.P., Delmer, C., Laurenzi, M.A., Hagos, M., et al., 2014. The East Africa Oligocene intertrappean beds: Regional distribution, depositional environments and Afro/Arabian mammal dispersals. J. Afr. Earth Sci. 99, 463–489.
Abebe, T., Balestrieri, M.L., Bigazzi, G., 2010. The Central Main Ethiopian rift is younger than 8 Ma: Confirmation through apatite fission-track thermochronology. Terra Nova 22 (6), 470–476.
Agostini, S., Di Giuseppe, P., Manetti, P., Doglioni, C., Conticelli, S., 2021. A heterogeneous subcontinental mantle under the African–Arabian Plate boundary revealed by boron and radiogenic isotopes. Sci. Rep. 11 (1), 11230.
Al Kwatli, M.A., Gillot, P.Y., Zeyen, H., Hildenbrand, A., Al Gharib, I., 2012. Volcano-tectonic evolution of the northern part of the Arabian plate in the light of new K–Ar ages and remote sensing: Harrat Ash Shaam volcanic province (Syria). Tectonophysics 580, 192–207.
Alemu, T., 2021. Tectonic evolution of the Pan-African Belt in Western Ethiopia, Southern Arabian-Nubian Shield. In: Hamimi, Z., et al. (Eds.), The Geology of the Arabian-Nubian Shield, Regional Geology Reviews, pp. 81–108.
Almond, D.C., 1986. Geological evolution of the Afro-Arabian dome. Tectonophysics 131, 301–332.
Alsharhan, A.S., Nairn, A.E.M., 1995. Tertiary of the Arabian Gulf: sedimentology and hydrocarbon potential. Palaeogeogr. Palaeoec. 114 (2–4), 369–384.
Andriampenomanana, F., Nyblade, A., Durrheim, R., Tugume, F., Nyago, J., 2021. Shear wave splitting measurements in northeastern Uganda and southeastern Tanzania: corroborating evidence for sublithospheric mantle flow beneath East Africa. Geophys. J. Int. 226 (3), 1696–1704.
ArRajehi, A., McClusky, S., Reilinger, R., Daoud, M., Alchalbi, A., Ergintav, S., et al., 2010. Geodetic constraints on present-day motion of the Arabian Plate: Implications for Red Sea and Gulf of Aden rifting. Tectonics 29 (3).
Auer, L., Boschi, L., Becker, T.W., Nissen-Meyer, T., Giardini, D., 2014. Savani: a variable resolution whole-mantle model of anisotropic shear velocity variations based on multiple data sets. *J. Geophys. Res.: Solid.* Earth 119 (4), 3006–3034.
Avigad, D., Gvirtzman, Z., 2009. Late Neoproterozoic rise and fall of the northern Arabian–Nubian Shield: the role of lithospheric mantle delamination and subsequent thermal subsidence. Tectonophysics 477 (3–4), 217–228.
Avni, Y., 1991. The geology, paleogeography and the landscape evolution of the Central Negev Highlands and the western Ramon structure. Isr. Geol. Surv. Rep. GSI/6/91, 153 pp.
Avni, Y., Segev, A., Ginat, H., 2012. Oligocene regional denudation of the northern Afar dome: Pre-and syn-breakup stages of the Afro-Arabian plate. Bulletin 124 (11–12), 1871–1897.
Bagley, B., Nyblade, A.A., 2013. Seismic anisotropy in eastern Africa, mantle flow, and the African superplume. Geophys. Res. Lett. 40 (8), 1500–1505.
Baker, J., Snee, L., Menzies, M., 1996. A brief Oligocene period of flood volcanism in Yemen. Earth Planet. Sci. Lett. 138, 39–55.
Ballato, P., Uba, C.E., Landgraf, A., Strecker, M.R., Sudo, M., Stockli, D.F., et al., 2011. Arabia-Eurasia continental collision: Insights from late Tertiary foreland-basin evolution in the Alborz Mountains, northern Iran. Bulletin 123 (1–2), 106–131.
Ballato, P., Parra, M., Schildgen, T.F., Dunkl, I., Yıldırım, C., Özsayın, E., Sobel, E.R., Echtler, H., Strecker, M.R., 2018. Multiple exhumation phases in the Central Pontides (N Turkey): New temporal constraints on major geodynamic changes associated with the closure of the Neo-Tethys Ocean. Tectonics 37 (6), 1831–1857.
Bar, O., Zilberman, E., 2016. Subsidence and conversion of the Dead Sea basin to an inland erosion base level in the early middle Miocene as inferred from geomorphological analysis of its ancient western fluvial outlet. Geomorphology 261, 147–161.
Bar, O., Gvirtzman, Z., Feinstein, S., Zilberman, E., 2013. Accelerated subsidence and sedimentation in the Levant Basin during the late Tertiary and concurrent uplift of

the Arabian platform: Tectonic versus counteracting sedimentary loading effects. Tectonics 32 (3), 334–350.
Bar, O., Zilberman, E., Feinstein, S., Calvo, R., Gvirtzman, Z., 2016. The uplift history of the Arabian Plateau as inferred from geomorphologic analysis of its northwestern edge. Tectonophysics 671, 9–23.
Barnett-Moore, N., Hassan, R., Flament, N., Müller, D., 2017. The deep Earth origin of the Iceland plume and its effects on regional surface uplift and subsidence. Sol. Ea. 8 (1), 235–254.
Barrier, E., Vrielynck, B., 2008. Palaeotectonic Maps of the Middle East. Atlas of, p. 14.
Bastow, I.D., Nyblade, A.A., Stuart, G.W., Rooney, T.O., Benoit, M.H., 2008. Upper mantle seismic structure beneath the Ethiopian hot spot: Rifting at the edge of the African low-velocity anomaly. Geochem. Geophys. Geosyst. 9, Q12022 https://doi.org/10.1029/2008GC002107.
Bastow, I.D., Pilidou, S., Kendall, J.M., Stuart, G.W., 2010. Melt-induced seismic anisotropy and magma assisted rifting in Ethiopia: evidence from surface waves. Geochem. Geophy. Geosyst. 11 (6).
Bartol, J., Govers, R., 2014. A single cause for uplift of the Central and Eastern Anatolian plateau? Tectonophysics 637, 116–136.
Bastow, I.D., Keir, D., Daly, E., 2011. The Ethiopia Afar Geoscientific Lithospheric Experiment (EAGLE): probing the transition from continental rifting to incipient sea floor spreading. Geol. Soc. Am., Soc. Pap. 478, ISSN, 1366–8781.
Becker, T.W., Lebedev, S., Long, M.D., 2012. On the relationship between azimuthal anisotropy from shear wave splitting and surface wave tomography. J. Geophys. Res. - Solid Earth 117, B01306. https://doi.org/10.1029/2011JB008705. Compilation updated in 05/2024, and available online at. http://www-udc.ig.utexas.edu/external/becker/sksdata.html. accessed 05/2024.
Becker, T.W., Faccenna, C., Humphreys, E.D., Lowry, A.R., Miller, M.S., 2014. Static and dynamic support of western U.S. topography. Earth Planet. Sci. Lett. 402, 234–246.
Bellahsen, N., Faccenna, C., Funiciello, F., Daniel, J.M., Jolivet, L., 2003. Why did Arabia separate from Africa? Insights from 3-D laboratory experiments. Earth Planet. Sci. Lett. 216 (3), 365–381. https://doi.org/10.1016/S0012-821X(03)00516-8.
Beltrandi, M.D., Pyre, A., 1973. Geological evolution of Southwest Somalia. Sedimentary Basins of the African Coasts 2, 159–178.
Ben-Israel, M., Matmon, A., Hidy, A.J., Avni, Y., Balco, G., 2020. Early-to-mid Miocene erosion rates inferred from pre-Dead Sea rift Hazeva River fluvial chert pebbles using cosmogenic 21 Ne. Earth. Surf. Dynam. 8 (2), 289–301.
Benoit, M.H., Nyblade, A.A., VanDecar, J.C., Gurrola, H., 2006a. Upper mantle P wave velocity structure and transition zone thickness beneath the Arabian Shield. Geophys. Res. Lett. 30 (10), 3–6. https://doi.org/10.1029/2002gl016436.
Benoit, M.H., Nyblade, A.A., Owens, T.J., Stuart, G., 2006b. Mantle transition zone structure and upper mantle S velocity variations beneath Ethiopia: evidence for a broad, deep-seated thermal anomaly. Geochem., Geophy., Geosy. 7 (11).
Berberian, M., 1995. Master "blind" thrust faults hidden under the Zagros folds: active basement tectonics and surface morphotectonics. Tectonophysics 241 (3–4), 193–224.
Berk Biryol, C., Beck, S.L., Zandt, G., Özacar, A.A., 2011. Segmented African lithosphere beneath the Anatolian region inferred from teleseismic P-wave tomography. Geophys. J. Int. 184 (3), 1037–1057.
Beydoun, Z.R., 1991. Arabian Plate Hydrocarbon Geology and Potential—A Plate Tectonic Approach. American Association of Petroleum Geologists.
Beydoun, Z.R., 1999. Evolution and development of the Levant (Dead Sea Rift) Transform System: a historical-chronological review of a structural controversy. Geol. Soc. Spec. Publ. 164 (1), 239–255.
Bonini, M., Corti, G., Innocenti, F., Manetti, P., Mazzarini, F., Abebe, T., Pecskay, Z., 2005. Evolution of the Main Ethiopian Rift in the frame of Afar and Kenya rifts propagation. Tectonics 24 (1).
Bookhagen, B., Thiede, R.C., Strecker, M.R., 2005. Abnormal monsoon years and their control on erosion and sediment flux in the high, arid northwest Himalaya. Earth Planet. Sci. Lett. 231 (1–2), 131–146.
Boone, S.C., Balestrieri, M.L., Kohn, B., 2021. Thermo-tectonic imaging of the Gulf of Aden-Red Sea rift systems and Afro-Arabian hinterland. Earth Sci. Rev. 222, 103824.
Bosworth, W., Stockli, D.F., 2016. Early magmatism in the greater Red Sea rift: timing and significance. Can. J. Earth Sci. 53 (11), 1158–1176.
Bosworth, W., Huchon, P., McClay, K., 2005. The red sea and gulf of Aden basins. J. Afr. Earth Sci. 43 (1–3), 334–378.
Bottrill, A.D., van Hunen, J., Allen, M.B., 2012. Insight into collision zone dynamics from topography: numerical modelling results and observations. Solid Earth 3 (2), 387–399.
Boyce, A., Bastow, I.D., Cottaar, S., Kounoudis, R., Guilloud De Courbeville, J., Caunt, E., Desai, S., 2021. AFRP20: New P-wavespeed model for the African mantle reveals two whole-mantle plumes below East Africa and neoproterozoic modification of the Tanzania Craton. Geochem., Geophy., Geosy. 22 (3) e2020GC009302.
Boyce, A., Kounoudis, R., Bastow, I.D., Cottaar, S., Ebinger, C.J., Ogden, C.S., 2023. Mantle wavespeed and discontinuity structure below East Africa: Implications for Cenozoic hotspot tectonism and the development of the Turkana Depression. Geochem. Geophys. Geosyst. 24 (8) e2022GC010775.
Braun, J., 2010. The many surface expressions of mantle dynamics. Nat. Geosci. 3 (12), 825.
Brew, G., Barazangi, M., Al-Maleh, A.K., Sawaf, T., 2001. Tectonic and geologic evolution of Syria. GeoArabia 6 (4), 573–616.
Brown, F.H., Mcdougall, I., 2011. Geochronology of the Turkana depression of northern Kenya and southern Ethiopia. Evol. Anthrop.: Issues, News, and Rev. 20 (6), 217–227.
Brown, G.F., Schmidt, D.L., Huffan, A.C., 1989. Geology of the Arabian Peninsula, Shield area of western Saudi Arabia. In: U.S. Geological Survey Professional Paper, 560-A.
Burke, K., 1996. The African plate. S. Afr. J. Geol. 99 (4), 341–409.
Burke, K., Gunnell, Y., 2008. The African erosion Surface: A Continental-Scale Synthesis of Geomorphology, Tectonics, and Environmental Change over the Past 180 Million Years. Soc. Am, Geol. https://doi.org/10.1130/MEM201.
Burke, K., Torsvik, T.H., 2004. Derivation of large igneous provinces of the past 200 million years from long-term heterogeneities in the deep mantle. Earth Planet. Sc. Lett. 227 (3–4), 531–538.
Burov, E., Gerya, T., 2014. Asymmetric three-dimensional topography over mantle plumes. Nature 513, 85–89.
Burov, E., Guillou-Frottier, L., 2005. The plume-head continental lithosphere interaction using a tectonically realistic formulation for the lithosphere. Geophys. J. Int. 58 https://doi.org/10.1111/j.136.-246x.2005.02588.x.
Burrough, P.A., McDonnell, R., 1998. Principles of Geographical Information Systems. Oxford University Press, Oxford, p. 333.
Camp, V.E., Roobol, M.J., 1992. Upwelling asthenosphere beneath western Arabia and its regional implications. *J. Geophys. Res.: Solid*. Earth 97 (B11), 15255–15271.
Cao, X., Flament, N., Müller, D., Li, S., 2018. The dynamic topography of eastern China since the latest Jurassic Period. Tectonics 37 (5), 1274–1291.
Cavazza, W., Cattò, S., Zattin, M., Okay, A.I., Reiners, P., 2018. Thermochronology of the Miocene Arabia-Eurasia collision zone of southeastern Turkey. Geosphere 14 (5), 2277–2293.
Cavazza, W., Albino, I., Galoyan, G., Zattin, M., Catto, S., 2019. Continental accretion and incremental deformation in the thermochronologic evolution of the Lesser Caucasus. Geosci. Front. 10 (6), 2189–2202. https://doi.org/10.1016/j.gsf.2019.02.007.
Chaimov, T.A., Barazangi, M., Al-Saad, D., Sawaf, T., Gebran, A., 1990. Crustal shortening in the Palmyride fold belt, Syria, and implications for movement along the Dead Sea fault system. Tectonics 9 (6), 1369–1386.
Champagnac, J.D., Schlunegger, F., Norton, K., von Blanckenburg, F., Abbühl, L.M., Schwab, M., 2009. Erosion-driven uplift of the modern Central Alps. Tectonophysics 474 (1–2), 236–249.
Chang, S.J., Van der Lee, S., 2011. Mantle plumes and associated flow beneath Arabia and East Africa. Earth Plan. Sci. Lett. 302 (3–4), 448–454.
Chang, S.-J., Merino, M., Van Der Lee, S., Stein, S., Stein, C.A., 2011. Mantle flow beneath Arabia offset from the opening Red Sea. Geophys. Res. Lett. 38 (4), 1–5. https://doi.org/10.1029/2010GL045852.
Chang, S.-J., Kendall, E., Davaille, A., Ferreira, A.M.G., 2020. The evolution of mantle plumes in East Africa. J. Geophys. Res. Solid Earth 125 (12). https://doi.org/10.1029/2020JB019929 e2020JB019929.
Chen, B., Kaban, M.K., El Khrepy, S., Al-Arifi, N., 2015. Effective elastic thickness of the Arabian plate: Weak shield versus strong platform. Geophys. Res. Lett. 42, 3298–3304. https://doi.org/10.1002/2015GL063725.
Civiero, C., Lebedev, S., Celli, N.L., 2022. A complex mantle plume head below East Africa-Arabia shaped by the lithosphere-asthenosphere boundary topography. Geochem., Geophy., Geosy. 23 https://doi.org/10.1029/2022GC010610 e2022GC010610.
Clementucci, R., Ballato, P., Siame, L., Fox, M., Lanari, R., Sembroni, A., , et al.Essaifi, A., 2023. Surface uplift and topographic rejuvenation of a tectonically inactive range: Insights from the Anti-Atlas and the Siroua Massif (Morocco). Tectonics 42 (2) e2022TC007383.
Cloetingh, S., Koptev, A., Lavecchia, A., Kovács, I.J., Beekman, F., 2022. Fingerprinting secondary mantle plumes. Earth Plan. Sci. Lett. 597, 117819 https://doi.org/10.1016/j.epsl.2022.117819.
Cloos, H., 1939. Hebung-Spaltung-Volcanismus. Geol. Rundsch. 30, 405–427.
Coleman, R.G., Gregory, R.T., Brown, G.F., 1983. Cenozoic Volcanic Rocks of Saudi Arabia, vol. 83. US Department of the Interior, Geological Survey. No. 788.
Coltorti, M., Dramis, F., Ollier, C.D., 2007. Planation surfaces in northern Ethiopia. Geomorphology 89 (3–4), 287–296.
Coltorti, M., Firuzabadi, D., Borri, A., Fantozzi, P., Pieruccini, P., 2015. Planation surfaces and the long-term geomorphological evolution of Ethiopia. Landscapes and landforms of Ethiopia 117–136.
Corti, G., 2009. Continental rift evolution: from rift initiation to incipient break-up in the Main Ethiopian Rift. East Africa. Earth-Sc. Rev. 96 (1–2), 1–53.
Courtillot, V., Jaupart, C., Manighetti, I., Tapponnier, P., Besse, J., 1999. On causal links between flood basalts and continental breakup. Earth Plan. Sci. Lett. 166 (3–4), 177–195.
Courtillot, V., Davaille, A., Besse, J., Stock, J., 2003. Three distinct types of hotspots in the Earth's mantle. Earth Plan. Sci. Lett. 205 (3–4), 295–308.
Cox, K.G., 1989. The role of mantle plumes in the development of continental drainage patterns. Nature 342 (6252), 873–877.
Crameri, F., Schmeling, H., Golabek, G.J., Duretz, T., Orendt, R., Buiter, S.J.H., Tackley, P.J., et al., 2012. A comparison of numerical surface topography calculations in geodynamic modelling: an evaluation of the 'sticky air' method. Geophys. J. Int. 189 (1), 38–54.
Czarnota, K., Roberts, G.G., White, N.J., Fishwick, S., 2014. Spatial and temporal patterns of Australian dynamic topography from River Profile Modeling. J. Geophys. Res.-Sol. Ea. 119 (2), 1384–1424.
d'Acremont, E., Leroy, S., Burov, E.B., 2003. Numerical modelling of a mantle plume: the plume head–lithosphere interaction in the formation of an oceanic large igneous province. Earth Planet. Sc. Lett. 206 (3–4), 379–396.
D'Agostino, N., McKenzie, D.P., 1999. Convective support of long wavelength topography in the Apennines (Italy). Terra Nova 11, 234–238.
Daradich, A., Mitrovica, J.X., Pysklywec, R.N., Willett, S.D., Forte, A.M., 2003. Mantle flow, dynamic topography, and rift-flank uplift of Arabia. Geology 31, 901–904.
Darin, M.H., Umhoefer, P.J., 2022. Diachronous initiation of Arabia–Eurasia collision from eastern Anatolia to the southeastern Zagros Mountains since middle Eocene

time. Int. Geol. Rev. 64 (18), 2653–2681. https://doi.org/10.1080/00206814.2022.2048272.
Davidson, A., 1983. Reconnaissance Geology and Geochemistry of Parts of Illubabor, Kefa, Gemu Gofa and Sidamo. Ethiopia, Ministry of Mines and Energy, Ethiopian Institute of Geological Surveys, Bulletin, p. 2.
Davidson, A., McGregor, D.C., 1976. Palynomorphs indicating Permian rocks in Ethiopia. Nature 262 (5567), 371–373.
Davila, F.M., Lithgow-Bertelloni, C., 2013. Dynamic topography in South America. J. South Am. Earth Sci. 43, 127–144.
Davison, I., Steel, I., 2018. Geology and hydrocarbon potential of the East African continental margin: a review. Pet. Geosci. 24 (1), 57–91.
de Vries, D., Heritage, S., Borths, M.R., Sallam, H.M., Seiffert, E.R., 2021. Widespread loss of mammalian lineage and dietary diversity in the early Oligocene of Afro-Arabia. Comm. Bio. 4 (1), 1172.
Debayle, E., Lévêque, J.J., Cara, M., 2001. Seismic evidence for a deeply rooted low-velocity anomaly in the upper mantle beneath the northeastern Afro/Arabian continent. Earth Plan. Sci. Lett. 193 (3–4), 423–436.
Demir, T., Westaway, R., Bridgland, D., Pringle, M., Yurtmen, S., Beck, A., Rowbotham, G., 2007. Ar-Ar dating of late Cenozoic basaltic volcanism in northern Syria: Implications for the history of incision by the River Euphrates and uplift of the northern Arabian Platform. Tectonics 26 (3).
Demir, T., Seyrek, A., Westaway, R., Bridgland, D., Beck, A., 2008. Late Cenozoic surface uplift revealed by incision by the River Euphrates at Birecik, Southeast Turkey. Quatern. Int. 186 (1), 132–163.
Dercourt, J.E.A., Zonenshain, L.P., Ricou, L.E., Kazmin, V.G., Le Pichon, X., Knipper, A. L., Biju-Duval, B., et al., 1986. Geological evolution of the Tethys belt from the Atlantic to the Pamirs since the Lias. Tectonophysics 123 (1–4), 241–315.
Dietz, R.S., Menard, H.W., 1953. Hawaiian swell, deep, and arch, and subsidence of the Hawaiian Islands. J. Geol. 61 (2), 99–113.
Dixon, T.H., Ivins, E.R., Franklin, B.J., 1989. Topographic and volcanic asymmetry around the Red Sea: Constraints on rift models. Tectonics 8 (6), 1193–1216.
Ebinger, C., 2005. Continental break-up: the East African perspective. Astron. Geophys. 46 (2), 2–16.
Ebinger, C., Sleep, N.H., 1998. Cenozoic magmatism in central and East Africa resulting from impact of one large plume. Nature 395, 788–791.
Ebinger, C.J., Forsyth, D.W., Bow, C.O., Bowin, C.O., 1989. Effective elastic plate thickness beneath the East African and Afar plateaus and dynamic compensation of the uplifts. J. Geophys. Res. 94 (B3), 2883–2901. https://doi.org/10.1029/jb094ib03p02883.
Ebinger, C.J., Reiss, M.C., Bastow, I., Karanja, M.M., 2024. Shallow sources of upper mantle seismic anisotropy in East Africa. Earth Planet. Sci. Lett. 625, 118488.
Emry, E.L., Shen, Y., Nyblade, A.A., Flinders, A., Bao, X., 2019. Upper mantle Earth structure in Africa from full-wave ambient noise tomography. Geochem. Geophys. Geosyst. 20 (1), 120–147.
Ernst, R.E., Youbi, N., 2017. How large Igneous Provinces affect global climate, sometimes cause mass extinctions, and represent natural markers in the geological record. Palaeogeogr. Palaeoec. 478, 30–52.
Ershov, A., Nikishin, A., 2004. Recent geodynamics of the Caucasus-Arabia-east Africa region. Geotectonics 38 (2), 123–136.
Faccenna, C., Becker, T.W., 2020. Topographic expressions of mantle dynamics in the Mediterranean. Earth-Sc. Rev. 209, 103327.
Faccenna, C., Bellier, O., Martinod, J., Piromallo, C., Regard, V., 2006. Slab detachment beneath eastern Anatolia: a possible cause for the formation of the North Anatolian fault. Earth Plan. Sci. Lett. 242 (1–2), 85–97.
Faccenna, C., Molin, P., Orecchio, B., Olivetti, V., Bellier, O., Funiciello, F., , et al.Billi, A., 2011. Topography of the Calabria subduction zone (southern Italy): Clues for the origin of Mt. Etna. *Tectonics* 30 (1).
Faccenna, C., Becker, T.W., Jolivet, L., Keskin, M., 2013. Mantle convection in the Middle East: Reconciling Afar upwelling, Arabia indentation and Aegean trench rollback. Earth Plan. Sci. Lett. 375, 254–269.
Faccenna, C., Glisovic, P., Forte, A., Becker, T.W., Garzanti, E., Sembroni, A., Gvirtzman, Z., 2019. Role of dynamic topography in sustaining the Nile River over 30 million years. Nat. Geosci. 12 (12).
Farnetani, C.G., Richards, M.A., 1994. Numerical investigations of the mantle plume initiation model for flood basalt events. J. Geophys. Res.-Sol. Ea. 99 (B7), 13813–13833.
Fielding, E.J., 1996. Tibet uplift and erosion. Tectonophysics 260 (1–3), 55–84.
Fishwick, S., 2010. Surface wave tomography: Imaging of the lithosphere-asthenosphere boundary beneath central and southern Africa? Lithos 120 (1–2), 63–73. https://doi.org/10.1016/j.lithos.2010.05.011.
Fishwick, S., Bastow, I.D., 2011. Towards a better understanding of African topography: a review of passive-source seismic studies of the African crust and upper mantle. Geol. Soc. Spec. Publ. 357 (1), 343–371.
Flament, N., Gurnis, M., Müller, R.D., 2013. A review of observations and models of dynamic topography. Lithos 5 (2), 189–210.
Forte, A.M., Quere, S., Moucha, R., Simmons, N.A., Grand, S.P., Mitrovica, J.X., Rowley, D.B., 2010. Joint seismic–geodynamic-mineral physical modelling of African geodynamics: a reconciliation of deep-mantle convection with surface geophysical constraints. Earth Plan. Sci. Lett. 295 (3–4), 329–341. https://doi.org/10.1016/j.epsl.2010.03.017.
French, S.W., Romanowicz, B., 2015. Broad plumes rooted at the base of the Earth's mantle beneath major hotspots. Nature 525, 95–99.
Freund, R., Garfunkel, Z., Zak, I., Goldberg, M., Weissbrod, T., Derin, B., Girdler, R.W., et al., 1970. The Shear along the Dead Sea Rift. Philosophical Transactions for the Royal Society of London. Series A, Mathematical and Physical Sciences, pp. 107–130.
Friedrich, A.M., 2019. Palaeogeological hiatus surface mapping: a tool to visualize vertical motion of the continents. Geol. Mag. 156 (2), 308–319.
Gaina, C., Van Hinsbergen, D.J., Spakman, W., 2015. Tectonic interactions between India and Arabia since the Jurassic reconstructed from marine geophysics, ophiolite geology, and seismic tomography. Tectonics 34 (5), 875–906.
Gani, N.D., 2015. Erosion history from incision modeling and river profile morphologies: example from the Tekeze River System, Ethiopian Plateau, East Africa. Arab. J. Geosci. 8, 11293–11305.
Gani, N.D., Neupane, P.C., 2018. Understanding transient landscape of the Ethiopian Plateau in relation to mantle dynamics. Geol. J. 53 (1), 371–385.
Gani, N.D., Gani, M.R., Abdelsalam, M.G., 2007. Blue Nile incision on the Ethiopian Plateau: Pulsed plateau growth, Pliocene uplift, and hominin evolution. GSA Today 17 (9), 4–11.
Gani, N.D., van Soest, M.C., Gani, M.R., Blackburn, N.C., Neupane, P., Bowden, S., Tadesse, K., 2023. Investigating apatite (U-Th)/he thermochronologic ages to understand exhumation history of the Ethiopian Plateau. J. Afr. Earth Sci. 198, 104605.
Garfunkel, Z., 1981. Internal structure of the Dead Sea leaky transform (rift) in relation to plate kinematics. Tectonophysics 80 (1–4), 81–108.
Garfunkel, Z., 1998. Constrains on the origin and history of the Eastern Mediterranean basin. Tectonophysics 298 (1–3), 5–35.
Garfunkel, Z., 1999. History and paleogeography during the Pan-African orogen to stable platform transition: Reappraisal of the evidence from the Elat area and the northern Arabian-Nubian Shield. Isr. J. Earth Sci. 48, 135–157.
Garfunkel, Z., 2002. Early Paleozoic Sediments of NE Africa and Arabia: Products of Continental-Scale erosion, Sediment Transport, and Deposition. Isr, J. Earth Sci, p. 51.
Garfunkel, Z., 2004. Origin of the Eastern Mediterranean basin: a reevaluation. Tectonophysics 391 (1–4), 11–34.
Garfunkel, Z., Horowitz, A., 1966. The Upper Tertiary and Quaternary morphology of the Negev. Isr. J. Earth Sci. 15, 101–117.
Garfunkel, Z., Zak, I., Freund, R., 1981. Active faulting in the Dead Sea rift. Tectonophysics 80 (1–4), 1–26.
Garzanti, E., Andò, S., Vezzoli, G., Megid, A.A.A., El Kammar, A., 2006. Petrology of Nile River sands (Ethiopia and Sudan): sediment budgets and erosion patterns. Earth Plan. Sci. Lett. 252 (3–4), 327–341.
Gibbons, A.D., Whittaker, J.M., Müller, R.D., 2013. The breakup of East Gondwana: Assimilating constraints from cretaceous ocean basins around India into a best-fit tectonic model. J. Geophys. Res.-Sol. Ea. 118 (3), 808–822.
Godard, V., Lavé, J., Carcaillet, J., Cattin, R., Bourlès, D., Zhu, J., 2010. Spatial distribution of denudation in Eastern Tibet and regressive erosion of plateau margins. Tectonophysics 491 (1–4), 253–274.
Göğüş, O.H., Pysklywec, R.N., 2008. Mantle lithosphere delamination driving plateau uplift and synconvergent extension in eastern Anatolia. Geology 36 (9), 723–726.
Griffiths, R.W., Campbell, I.H., 1991. Interaction of mantle plume heads with the Earth's surface and onset of small-scale convection. J. Geophys. Res.-Sol. Ea. 96 (B11), 18295–18310.
Guiraud, R., Bosworth, W., Thierry, J., Delplanque, A., 2005. Phanerozoic geological evolution of Northern and Central Africa: an overview. J. Afr. Earth Sci. 43 (1–3), 83–143.
Gurnis, M., Mitrovica, J.X., Ritsema, J., van Heijst, H.J., 2000. Constraining mantle density structure using geological evidence of surface uplift rates: the case of the African Superplume. Geochem. Geophys. Geosyst. 1, 1020. https://doi.org/10.1029/1999GC000035.
Gusmeo, T., Cavazza, W., Alania, V.M., Enukidze, O.V., Zattin, M., Corrado, S., 2021. Structural inversion of back-arc basins – the Neogene Adjara-Trialeti fold-and-thrust belt (SW Georgia) as a far-field effect of the Arabia-Eurasia collision. Tectonophysics 803, 228702. https://doi.org/10.1016/j.tecto.2020.228702.
Gvirtzman, Z., Zilberman, E., Folkman, Y., 2008. Reactivation of the Levant passive margin during the late Tertiary and formation of the Jaffa Basin offshore Central Israel. J. Geol. Soc. London 165 (2), 563–578.
Gvirtzman, Z., Steinberg, J., Bar, O., Buchbinder, B., Zilberman, E., Siman-Tov, R., Rosensaft, M., et al., 2011. Retreating late Tertiary shorelines in Israel: Implications for the exposure of North Arabia and Levant during Neotethys closure. Lithosphere 3 (2), 95–109.
Gvirtzman, Z., Faccenna, C., Becker, T.W., 2016. Isostasy, flexure, and dynamic topography. Tectonophysics 683, 255–271.
Hager, B.H., Clayton, R.W., Richards, M.A., Comer, R.P., Dzievonski, A.M., 1985. Lower mantle heterogeneity, dynamic topography and the geoid. Nature 313 (6003), 541.
Hammond, J.O.S., Kendall, J.-M., Wookey, J., Stuart, G.W., Keir, D., Ayele, A., 2014. Differentiating flow, melt, or fossil seismic anisotropy beneath Ethiopia. Geochem. Geophys. Geosyst. 15, 1878–1894. https://doi.org/10.1002/2013GC005185.
Hansen, S.E., Nyblade, A.A., 2013. The deep seismic structure of the Ethiopia/Afar hotspot and the African superplume. Geophys. J. Int. 194 (1), 118–124.
Hansen, S.E., Nyblade, A.A., Benoit, M.H., 2012. Mantle structure beneath Africa and Arabia from adaptively parameterized P-wave tomography: Implications for the origin of Cenozoic Afro-Arabian tectonism. Earth Plan. Sci. Lett. 319, 23–34. https://doi.org/10.1016/j.epsl.2011.12.023.
Hansen, S., Schwartz, S., Al-Amri, A., Rodgers, A., 2006. Combined plate motion and density-driven flow in the asthenosphere beneath Saudi Arabia: evidence from shear-wave splitting and seismic anisotropy. Geology 34 (10), 869–872. https://doi.org/10.1130/g22713.1.
Hartmann, J., Moosdorf, N., 2012. The new global lithological map database GLiM: a representation of rock properties at the Earth surface. Geochem. Geophys. Geosyst. 13 (12).

Heller, P.L., Liu, L., 2016. Dynamic topography and vertical motion of the US Rocky Mountain region prior to and during the Laramide orogeny. Bulletin 128 (5–6), 973–988.
Heron, P.J., 2018. Mantle Plumes and Mantle Dynamics in the Wilson Cycle. *In*: Wilson, R.W., Houseman, G.A., Mccaffrey, K.J.W., Dor'e, a.G., Buiter, S.J.H. (Eds.), Fifty Years of the Wilson Cycle Concept in Plate Tectonics. Geol. Soc. Spec. Publ, p. 470. https://doi.org/10.1144/SP470.18.
Hessami, K., Koyi, H.A., Talbot, C.J., Tabasi, H., Shabanian, E., 2001. Progressive unconformities within an evolving foreland fold–thrust belt. Zagros Mountains. J. Geol. Soc. 158 (6), 969–981.
Hofmann, C., Courtillot, V., Feraud, G., Rochette, P., Yirgu, G., Ketefo, E., Pik, R., 1997. Timing of the Ethiopian flood basalt event and implications for plume birth and global change. Nature 389, 838–841.
Hoke, G., Isacks, L., Jordan, T.E., 2005. Equilibrium landscapes of the western Andean mountain front (10°S - 33°S): Long-term responses to along-strike changes in climate. In: 6th International Symposium on Andean Geodynamics (ISAG 2005, Barcelona), Extended Abstracts, pp. 386–389.
Hosseini, K., Sigloch, K., Tsekhmistrenko, M., Zaheri, A., Nissen-Meyer, T., Igel, H., 2020. Global mantle structure from multifrequency tomography using P, PP and P-diffracted waves. Geophys. J. Int. 220 (1), 96–141.
Houseman, G.A., 1990. The thermal structure of mantle plumes: axisymmetric or triple-junction? Geophys. J. Int. 102 (1), 15–24.
Hua, J., Fischer, K.M., Gazel, E., Parmentier, E.M., Hirth, G., 2023. Long-distance asthenospheric transport of plume-influenced mantle from Afar to Anatolia. Geochem. Geophys. Geosyst. 24 https://doi.org/10.1029/2022GC010605 e2022GC010605.
Hunegnaw, A., Sage, L., Gonnard, R., 1998. Hydrocarbon potential of the intracratonic Ogaden Basin. SE Ethiopia. *J. Petrol. Geol.* 21 (4), 401–425.
Ilani, S., Harlavan, Y., Tarawneh, K., Rabba, I., Weinberger, R., Ibrahim, K., , et al. Steinitz, G., 2001. New K-Ar ages of basalts from the Harrat Ash Shaam volcanic field in Jordan: Implications for the span and duration of the upper-mantle upwelling beneath the western Arabian plate. Geology 29 (2), 171–174.
Isacks, B.L., 1992. Long Term Land Surface Processes: Erosion, Tectonics and climate history in Mountain Belts. In: Mather, P. (Ed.), TERRA-1, Understanding the Terrestrial Environment. Taylor and Francis, London, UK, pp. 21–36.
Ismail, E.H., Abdelsalam, M.G., 2012. Morpho-tectonic analysis of the Tekeze River and the Blue Nile drainage systems on the Northwestern Plateau. Ethiopia. *J. Afr. Earth Sci.* 69, 34–47.
Joffe, S., Garfunkel, Z., 1987. Plate kinematics of the circum Red Sea—a re-evaluation. Tectonophysics 141 (1–3), 5–22.
Johnson, P.R., 2003. Post-amalgamation basins of the NE Arabian shield and implications for neoproterozoic III tectonism in the northern East African orogen. Precambrian Res. 123, 321–337.
Johnson, P.R., Zoheir, B.A., Ghebreab, W., Stern, R.J., Barrie, C.T., Hamer, R.D., 2017. Gold-bearing volcanogenic massive sulfides and orogenic-gold deposits in the Nubian Shield. S. Afr. J. Geol. 120 (1), 63–76.
Jones, S.M., Lovell, B., Crosby, A.G., 2012. Comparison of modern and geological observations of dynamic support from mantle convection. J. Geol. Soc. London 169 (6), 745–758.
Kendall, J.M., Stuart, G.W., Ebinger, C.J., Bastow, I.D., Keir, D., 2005. Magma-assisted rifting in Ethiopia. Nature 433 (7022), 146–148.
Keskin, M., 2003. Magma generation by slab steepening and breakoff beneath a subduction-accretion complex: an alternative model for collision-related volcanism in Eastern Anatolia. Turkey. Geophys. Res. Lett. 30 (24).
Keskin, M., 2007. In: Foulger, G.R., Jurdy, D.M. (Eds.), Plates, Plumes, and Planetary Processes, Vol. 430,. Geological Society of America, pp. 693–722.
Khalil, H.M., Capitanio, F.A., Betts, P.G., Cruden, A.R., 2020. 3-D analog modeling constraints on rifting in the Afar region. Tectonics 39 (10) e2020TC006339.
Kieffer, B., Arndt, N., Lapierre, H., Bastien, F., Bosch, D., Pecher, A., , et al.Meugniot, C., 2004. Flood and shield basalts from Ethiopia: magmas from the African superswell. J. Petrol. 45 (4), 793–834. https://doi.org/10.1093/petrology/egg112.
Kiraly, A., Faccenna, C., Funiciello, F., Sembroni, A., 2015. Coupling surface and mantle dynamics: a novel experimental approach. Geophys. Res. Lett. 42 (10), 3863–3869.
Kohn, B.P., Eyal, M., Feinstein, S., 1992. A major late Devonian-early Carboniferous (Hercynian) Thermotectonic event at the NW margin of the Arabian-Nubian Shield: evidence from zircon fission track dating. Tectonics 11 (5), 1018–1027.
Koppers, A., Becker, T.W., Jackson, M., Konrad, K., Müller, R.D., Romanowicz, B., Steinberger, B., Whittaker, J., 2021. Mantle plumes and their role in Earth processes. Nature Rev. Earth & Environ. 2, 382–401.
Koptev, A., Calais, E., Burov, E., Leroy, S., Gerya, T., 2015. Dual continental rift systems generated by plume–lithosphere interaction. Nat. Geosci. 8 (5), 388–392.
Koptev, A., Cloetingh, S., Burov, E., François, T., Gerya, T., 2017. Long-distance impact of Iceland plume on Norway's rifted margin. Sci. Rep. 7 (1), 10408.
Koptev, A., Burov, E., Gerya, T., Le Pourhiet, L., Leroy, S., Calais, E., Jolivet, L., 2018. Plume-induced continental rifting and break-up in ultra-slow extension context: Insights from 3D numerical modeling. Tectonophysics 746, 121–137.
Koshnaw, R.I., Stockli, D.F., Schlunegger, F., 2019. Timing of the Arabia-Eurasia continental collision—evidence from detrital zircon U-Pb geochronology of the Red Bed Series strata of the northwest Zagros hinterland. Kurdistan region of Iraq. Geology 47 (1), 47–50.
Koulakov, I., Burov, E., Cloetingh, S., El Khrepy, S., Al-Arifi, N., Bushenkova, N., 2016. Evidence for anomalous mantle upwelling beneath the Arabian Platform from travel time tomography inversion. Tectonophysics 667, 176–188. https://doi.org/10.1016/j.tecto.2015.11.022.
Kounoudis, R., Bastow, I.D., Ebinger, C.J., Darbyshire, F., Ogden, C.S., Musila, M., Ugo, F., Ayele, A., Sullivan, G., Bendick, R., Mariita, N., Kianji, G., 2023. The development of rifting and magmatism in the multiply rifted Turkana Depression, East Africa: Evidence from surface-wave analysis of crustal and uppermost mantle structure. Earth and Planetary Science Letters 621, 118386.
Kounoudis, R., Bastow, I.D., Ogden, C.S., Goes, S., Jenkins, J., Grant, B., Braham, C., 2020. Seismic tomographic imaging of the Eastern Mediterranean mantle: implications for terminal-stage subduction, the uplift of Anatolia, and the development of the North Anatolian Fault. Geochemistry, Geophysics, Geosystems 21 (7), e2020GC009009.
Krenkel, E., 1924. Der Syrische Bogen. *Zentralblatt Mineralogie* 9 (10), 274–281.
Krienitz, M.S., Haase, K.M., Mezger, K., van den Bogaard, P., Thiemann, V., Shaikh-Mashail, M.A., 2009. Tectonic events, continental intraplate volcanism, and mantle plume activity in northern Arabia: Constraints from geochemistry and Ar-Ar dating of Syrian lavas. Geochem. Geophys., Geosy. 10 (4).
Kühni, A., Pfiffner, O.A., 2001. The relief of the Swiss Alps and adjacent areas and its relation to lithology and structure: topographic analysis from a 250-m DEM. Geomorphology 41 (4), 285–307.
Lanari, R., Boutoux, A., Faccenna, C., Herman, F., Willett, S.D., Ballato, P., 2023. Cenozoic exhumation in the Mediterranean and the Middle East. Earth-Sc. Rev. 237, 104328.
Laske, G., Masters, G., Ma, Z., Pasyanos, M., 2013. Update on CRUST1. 0—A 1-degree global model of Earth's. In: Geophysical Research Abstracts, vol. 15. EGU General Assembly, Vienna, Austria, p. 2658. No. 15.
Lebkicher, R., 1960. Aramco Handbook. Arabian American Oil Company.
Leroy, S., Razin, P., Autin, J., Bache, F., Acremont, E., Watremez, L., Lazki, A.A., et al., 2012. From rifting to oceanic spreading in the Gulf of Aden: a synthesis. Arab. J. Geosci. 5, 859–901.
Lim, J.A., Chang, S.J., Mai, P.M., Zahran, H., 2020. Asthenospheric flow of plume material beneath Arabia inferred from S wave traveltime tomography. J. Geophys. Res.-Sol. Ea. 125 (8) https://doi.org/10.1029/2020JB019668.
Lithgow-Bertelloni, C., Silver, P.G., 1998. Dynamic topography, plate driving forces and the African superswell. Nature 395, 269–272. https://doi.org/10.1038/26212.
Liu, L., 2015. The ups and downs of North America: evaluating the role of mantle dynamic topography since the Mesozoic. Rev. Geophys. 53 (3), 1022–1049.
Lu, C., Grand, S.P., Lai, H., Garnero, E.J., 2019. TX2019slab: a new P and S tomography model incorporating subducting slabs. *J. Geophys. Res.: Solid.* Earth 124 (11), 11549–11567.
Lustrino, M., Wilson, M., 2007. The circum-Mediterranean anorogenic Cenozoic igneous province. Earth-Sc. Rev. 81 (1–2), 1–65.
Macgregor, D., 2015. History of the development of the East African Rift System: a series of interpreted maps through time. J. Afr. Earth Sci. 101, 232–252.
Macgregor, D., 2018. History of the development of Permian–Cretaceous rifts in East Africa: a series of interpreted maps through time. Petrol. Geosci. 24 (1), 8–20.
Mackenzie, G.H., Thybo, H., Maguire, P., 2005. Crustal velocity structure across the Main Ethiopian Rift: results from two-dimensional wide-angle seismic modelling. Geophys. J. Int. 162, 994–1006.
McClusky, S., Reilinger, R., Mahmoud, S., Ben Sari, D., Tealeb, A., 2003. GPS constraints on Africa (Nubia) and Arabia plate motions. Geophys. J. Int. 155 (1), 126–138.
McClusky, S., Reilinger, R., Ogubazghi, G., Amleson, A., Healeb, B., Vernant, P., , et al. Kogan, L., 2010. Kinematics of the southern Red Sea–Afar Triple Junction and implications for plate dynamics. Geophys. Res. Lett. 37 (5).
McDougall, I., Morton, W.H., William, M.A.J., 1975. Ages and rates of denudation of trap series basalts at the Blue Nile Gorge, Ethiopia. Nature 254, 207–209.
McKenzie, D., 1984. A possible mechanism for epeirogenic uplift. Nature 307 (5952), 616–618.
McQuarrie, N., Stock, J., Verdel, C., Wernicke, B., 2003. Cenozoic evolution of Neotethys and implications for the causes of plate motions. Geophys. Res. Lett. 30 (20), 2036. https://doi.org/10.1029/2003GL017992.
Mège, D., Purcell, P., Pochat, S., Guidat, T., 2015. The landscape and landforms of the Ogaden, Southeast Ethiopia. Landscapes and landforms of Ethiopia 323–348.
Mège, D., Purcell, P., Bézos, A., Jourdan, F., La, C., 2016. A major dyke swarm in the Ogaden region south of Afar and the early evolution of the Afar triple junction. Geol. Soc. Spec. Publ. 420 (1), 221–248.
Memiş, C., Göğüş, O.H., Uluocak, E.Ş., Pysklywec, R., Keskin, M., Şengör, A.C., Topuz, G., 2020. Long wavelength progressive plateau uplift in Eastern Anatolia since 20 Ma: implications for the role of slab peel-Back and Break-off. Geochem. Geophys. Geosy. 21 (2) e2019GC008726.
Molin, P., Pazzaglia, F.J., Dramis, F., 2004. Geomorphic expression of active tectonics in a rapidly-deforming forearc, Sila massif, Calabria, southern Italy. Am. J. Sci. 304 (7), 559–589.
Merry, T.A., Bastow, I.D., Kounoudis, R., Ogden, C.S., Bell, R.E., Jones, L., 2021. The influence of the North Anatolian Fault and a fragmenting slab architecture on upper mantle seismic anisotropy in the eastern Mediterranean. Geochemistry, Geophysics, Geosystems 22 (9), e2021GC009896.
Molin, P., Fubelli, G., Nocentini, M., Sperini, S., Ignat, P., Grecu, F., Dramis, F., 2012. Interaction of mantle dynamics, crustal tectonics and surface processes in the topography of the Romanian Carpathians: a geomorphological approach. Global Planet. Change. https://doi.org/10.1016/j.gloplacha.2011.05.005.
Molin, P., Sembroni, A., Ballato, P., Faccenna, C., 2023. The uplift of an early stage collisional plateau unraveled by fluvial network analysis and river longitudinal profile inversion: the case of the Eastern Anatolian Plateau. Tectonics 42. https://doi.org/10.1029/2022TC007737 e2022TC007737.
Montagner, J.P., Marty, B., Stutzmann, E., Sicilia, D., Cara, M., Pik, R., Debayle, E., et al., 2007. Mantle upwellings and convective instabilities revealed by seismic tomography and helium isotope geochemistry beneath eastern Africa. Geophys. Res. Lett. 34 (21).

Montelli, R., Nolet, G., Dahlen, F.A., Masters, G., 2006. A catalogue of deep mantle plumes: New results from finite-frequency tomography. Geochem. Geophys. Geosy. 7 (11).

Moucha, R., Forte, A.M., 2011. Changes in African topography driven by mantle convection. Nat. Geosci. 4 (10), 707–712.

Moucha, R., Forte, A.M., Mitrovica, J.X., Rowley, D.B., Quéré, S., Simmons, N.A., Grand, S.P., 2008. Dynamic topography and long-term sea-level variations: there is no such thing as a stable continental platform. Earth Planet. Sci. Lett. 271 (1–4), 101–108. https://doi.org/10.1016/j.epsl.2008.03.056.

Mukhopadhyay, M., Mukhopadhyay, B., Mogren, S., Nandi, B.K., Varghese, S., Ibrahim, E., 2023. Geophysical modelling detects an intrusive magmatic body in the lower crust atop an underplated Moho at the Red Sea rifted margin, Central Saudi Arabia. J. Afr. Earth Sci. 202, 104914.

Murris, R.J., 1980. Middle East: stratigraphic evolution and oil habitat. AAPG Bull. 64 (5), 597–618.

Nelson, W.R., Furman, T., van Keken, P.E., Shirey, S.B., Hanan, B.B., 2012. OsHf isotopic insight into mantle plume dynamics beneath the East African Rift System. Chem. Geol. 320, 66–79.

Nuriel, P., Weinberger, R., Kylander-Clark, A.R.C., Hacker, B.R., Craddock, J.P., 2017. The onset of the Dead Sea transform based on calcite age-strain analyses. Geology 45 (7), 587–590.

Nyblade, A.A., 2011. The upper-mantle low-velocity anomaly beneath Ethiopia, Kenya, and Tanzania: Constraints on the origin of the African superswell in eastern Africa and plate versus plume models of mantle dynamics. Geol. Soc. Am. Spec. Paper 478, 37–50.

Nyblade, A.A., Owens, T.J., Gurrola, H., Ritsema, J., Langston, C.A., 2000. Seismic evidence for a deep upper mantle thermal anomaly beneath East Africa. Geology 28 (7), 599–602.

Ogden, C.S., Bastow, I.D., 2022. The crustal structure of the Anatolian Plate from receiver functions and implications for the uplift of the central and eastern Anatolian plateaus. Geophysical Journal International 229 (2), 1041–1062.

Okay, A.I., Zattin, M., Cavazza, W., 2010. Apatite fission-track data for the Miocene Arabia-Eurasia collision. Geology 38 (1), 35–38. https://doi.org/10.1130/G30234.1.

Padoan, M., Garzanti, E., Harlavan, Y., Villa, I.M., 2011. Tracing nile sediment sources by Sr and Nd isotope signatures (Uganda, Ethiopia, Sudan). Geochim. Cosmochim. Acta 75 (12), 3627–3644.

Panasyuk, S.V., Hager, B.H., 2000. Models of isostatic and dynamic topography, geoid anomalies, and their uncertainties. J. Geophys. Res.-Sol. Ea. 105 (B12), 28199–28209.

Paul, J.D., Roberts, G.G., White, N., 2014. The African landscape through space and time. Tectonics 33 (6), 898–935.

Picard, L., 1951. Geomorphogeny of Israel, part 1 — the Negev. Bull. Res. Counc. Isr. 1 (1–2), 1–32.

Pik, R., Marty, B., Carignan, J., Lavé, J., 2003. Stability of the Upper Nile drainage network (Ethiopia) deduced from (U–Th)/he thermochronometry: implications for uplift and erosion of the Afar plume dome. Earth Plan. Sci. Lett. 215 (1–2), 73–88.

Pik, R., Bellahsen, N., Leroy, S., Denèle, Y., Razin, P., Ahmed, A., Khanbari, K., 2013. Structural control of basement denudation during rifting revealed by low-temperature (U–Th–Sm)/he thermochronology of the Socotra Island basement—Southern Gulf of Aden margin. Tectonophysics 607, 17–31.

Pirouz, M., Avouac, J.P., Hassanzadeh, J., Kirschvink, J.L., Bahroudi, A., 2017. Early Neogene foreland of the Zagros, implications for the initial closure of the Neo-Tethys and kinematics of crustal shortening. Earth Plan. Sci. Lett. 477, 168–182.

Powers, R.W., Ramirez, L.F., Redmond, C.D., Elberg Jr., E.L., 1966. Geology of the Arabian Peninsula: Sedimentary geology of Saudi Arabia (No. 560-D). US Geological Survey.

Prave, A.R., Bates, C.R., Donaldson, C.H., Toland, H., Condon, D.J., Mark, D., Raub, T.D., 2016. Geology and geochronology of the Tana Basin, Ethiopia: LIP volcanism, super eruptions and Eocene–Oligocene environmental change. Earth Plan. Sci. Lett. 443, 1–8.

Priestley, K., McKenzie, D., Debayle, E., Pilidou, S., 2008. The African upper mantle and its relationship to tectonics and surface geology. Geophys. J. Int. 175 (3), 1108–1126.

Purcell, P.G., 2017. Re-imagining and re-imaging the development of the East African Rift. Pet. Geosci. 24 (1), 21–40.

Qaysi, S., Liu, K.H., Gao, S.S., 2018. A database of shear-wave splitting measurements for the Arabian Plate. Seismol. Res. Lett. 89 (6), 2294–2298. https://doi.org/10.1785/0220180144.

Quennell, A.M., 1958. The structural and geomorphic evolution of the Dead Sea Rift. Quat. J. Geol. Soc. Lond. 114, 1–24.

Reeves, C., De Wit, M., 2000. Making ends meet in Gondwana: retracing the transforms of the Indian Ocean and reconnecting continental shear zones. Terra Nova 12 (6), 272–280.

Reilinger, R., McClusky, S., 2011. Nubia–Arabia–Eurasia plate motions and the dynamics of Mediterranean and Middle East tectonics. Geophys. J. Int. 186 (3), 971–979.

Reilinger, R., McClusky, S., Vernant, P., Lawrence, S., Ergintav, S., Cakmak, R., , et al. Karam, G., 2006. GPS constraints on continental deformation in the Africa-Arabia-Eurasia continental collision zone and implications for the dynamics of plate interactions. J. Geophys. Res.-Sol. Ea. 111 (B5).

Reiss, M.C., Long, M.D., Creasy, N., 2019. Lowermost mantle anisotropy beneath Africa from differential SKS-SKKS shear-wave splitting. *J. Geophys. Res.: Solid.* Earth 124 (8), 8540–8564.

Ribe, N.M., Christensen, U.R., 1994a. Three-dimensional modeling of plume-lithosphere interaction. J. Geophys. Res.-Sol. Ea. 99 (B1), 669–682.

Ribe, N.M., Christensen, U.R., 1994b. Three-dimensional modeling of plume-lithosphere interaction. J. Geophys. Res. Solid Earth 99, 669–682.

Ribe, N.M., Christensen, U.R., 1999. The dynamical origin of Hawaiian volcanism. Earth Plan. Sci. Lett. 171 (4), 517–531.

Richards, M.A., Hager, B.H., Sleep, N.H., 1988. Dynamically supported geoid highs over hotspots: Observation and theory. J. Geophys. Res. Solid Earth 93, 7690–7708.

Richards, M.A., Duncan, R.A., Courtillot, V.E., 1989. Flood basalts and hot-spot tracks: plume heads and tails. Science 246, 103–107.

Ritsema, J., van Heijst, H., 2000. New seismic model of the upper mantle beneath Africa. Geology 28 (1), 63–66.

Ritsema, J., van Heijst, H.J., Woodhouse, J.H., 1999. Complex shear wave velocity structure imaged beneath Africa and Iceland. Science 286, 1925–1928. https://doi.org/10.1126/science.286.5446.1925.

Roberts, G.G., White, N., 2010. Estimating uplift rate histories from river profiles using African examples. J. Geophys. Res.-Sol. Ea. 115 (B2).

Roberts, G.G., Paul, J.D., White, N., Winterbourne, J., 2012. Temporal and spatial evolution of dynamic support from river profiles: a framework for Madagascar. Geochem. Geophys. Geosyst. 13 (4).

Robertson, A.H.F., Dixon, J.E., 1984. Introduction: aspects of the geological evolution of the Eastern Mediterranean. Geol. Soc. Spec. Publ. 17 (1), 1–74.

Robertson, A.H., Ustaömer, T., Parlak, O., Ünlügenç, U.C., Taşlı, K., Inan, N., 2006. The Berit transect of the Tauride thrust belt, S Turkey: Late Cretaceous–Early Cenozoic accretionary/collisional processes related to closure of the Southern Neotethys. J. Asian Earth Sci. 27 (1), 108–145.

Robinet, J., Razin, P., Serra-Kiel, J., Gallardo-Garcia, A., Leroy, S., Roger, J., Grelaud, C., 2013. The Paleogene pre-rift to syn-rift succession in the Dhofar margin (northeastern Gulf of Aden): stratigraphy and depositional environments. Tectonophysics 607, 1–16.

Rogers, N.W., 2006. Basaltic magmatism and the geodynamics of the East African Rift System. Geological Society, London, Special Publications 259 (1), 77–93.

Rogers, N., Macdonald, R., Fitton, J., George, R., Smith, R., Barreiro, B., 2000. Two mantle plumes beneath the East African rift system: Sr, Nd and Pb isotope evidence from Kenya Rift basalt. Earth Planet. Sci. Lett. 176, 387–400.

Rooney, T.O., 2017. The Cenozoic magmatism of East-Africa: Part I—flood basalts and pulsed magmatism. Lithos 286, 264–301.

Rooney, T.O., Mohr, P., Dosso, L., Hall, C., 2013. Geochemical evidence of mantle reservoir evolution during progressive rifting along the western Afar margin. Geochim. Cosmochim. Acta 102, 65–88.

Rowley, D.B., Forte, A.M., Moucha, R., Mitrovica, J.X., Simmons, N.A., Grand, S.P., 2013. Dynamic topography change of the eastern United States since 3 million years ago. Science 340 (6140), 1560–1563.

Roy, M., Jordan, T.H., Pederson, J., 2009. Colorado Plateau magmatism and uplift by warming of heterogeneous lithosphere. Nature 459 (7249), 978–982.

Rubey, M., Brune, S., Heine, C.J., Davies, R.D., Williams, S.E., Muller, R.D., 2017. Global patterns in Earth's dynamic topography since the Jurassic: the role of subducted slabs. Sol. Ea. 8, 899–919. https://doi.org/10.5194/se-8-899-2017.

Saeidi, H., Hansen, S.E., Nyblade, A.A., 2023. Deep mantle influence on the Cameroon Volcanic Line. Geochem. Geophy., Geosy. 24 (1) e2022GC010621.

Salameh, H.R., 1997. Geomorphology of the eastern coast of the Dead Sea, Jordan. Geo Journal 41, 255–266.

Schaeffer, A.J., Lebedev, S., 2013. Global shear speed structure of the upper mantle and transition zone. Geophys. J. Int. 194 (1), 417–449.

Schildgen, T.F., Yıldırım, C., Cosentino, D., Strecker, M.R., 2014. Linking slab break-off, Hellenic trench retreat, and uplift of the Central and Eastern Anatolian plateaus. Earth-Sc. Rev. 128, 147–168.

Sella, G.F., Dixon, T.H., Mao, A., 2002. REVEL: a model for recent plate velocities from space geodesy. J. Geophys. Res.-Sol. Ea. 107 (B4), ETG–11.

Sembroni, A., Molin, P., 2018. Long-term drainage system evolution in the Wabe Shebele River basin (SE Ethiopia-SW Somalia). Geomorphology 320, 45–63.

Sembroni, A., Faccenna, C., Becker, T.W., Molin, P., Abebe, B., 2016a. Long-term, deep-mantle support of the Ethiopia-Yemen Plateau. Tectonics 35 (2), 469–488.

Sembroni, A., Molin, P., Pazzaglia, F.J., Faccenna, C., Abebe, B., 2016b. Evolution of continental-scale drainage in response to mantle dynamics and surface processes: an example from the Ethiopian Highlands. Geomorphology 261, 12–29.

Sembroni, A., Kiraly, A., Faccenna, C., Funiciello, F., Becker, T.W., Globig, J., Fernandez, M., 2017. Impact of the lithosphere on dynamic topography: Insights from analogue modeling. Geophys. Res. Lett. 44 (6), 2693–2702.

Sembroni, A., Molin, P., Faccenna, C., 2021. Drainage system organization after mantle plume impingement: the case of the Horn of Africa. Earth-Sc. Rev. 216, 103582.

Sengör, A.M.C., 2001. Elevation as indicator of mantle-plume activity. *Geol. Soc. Am.* Spec. Pap. 352, 183–225.

Şengör, A.M.C., Özeren, S., Genç, T., Zor, E., 2003. East Anatolian high plateau as a mantle-supported, north-south shortened domal structure. Geophys.Res. Lett. 30 (24).

Şengör, A.M.C., Tüysüz, O., Imren, C., Sakınç, M., Eyidoğan, H., Görür, N., Rangin, C., et al., 2005. The North Anatolian fault: a new look. Annu. Rev. Earth Planet. Sci. 33, 37–112.

Şengül Uluocak, E., Göğüş, O.H., Pysklywec, R.N., Chen, B., 2021. Geodynamics of East Anatolia-caucasus domain: inferences from 3D thermo-mechanical models, residual topography, and admittance function analyses. Tectonics 40 (12), e2021TC007031.

Seward, D., Grujic, D., Schreurs, G., 2004. An insight into the breakup of Gondwana: Identifying events through low-temperature thermochronology from the basement rocks of Madagascar. Tectonics 23 (3).

Sicilia, D., Montagner, J.P., Cara, M., Stutzmann, E., Debayle, E., Lépine, J.C., Sholan, J. M., et al., 2008. Upper mantle structure of shear-waves velocities and stratification of anisotropy in the Afar Hotspot region. Tectonophysics 462 (1–4), 164–177.

Sreenidhi, K.S., Betts, P.G., Radhakrishna, M., Armit, R., 2023. Influence of lateral plume channel on the evolution of rift arms of the afar triple junction: constraints from 3-D gravity interpretation. Journal of Geophysical Research: Solid Earth 128 (8), e2023JB026791.

Steinberger, B., 2016. Topography caused by mantle density variations: observation-based estimates and models derived from tomography and lithosphere thickness. Geophysical Supplements to the Monthly Notices of the Royal Astronomical Society 205 (1), 604–621.

Steinberger, B., Bredow, E., Lebedev, S., Schaeffer, A., Torsvik, T.H., 2019. Widespread volcanism in the Greenland–North Atlantic region explained by the Iceland plume. Nat. Geosci. 12 (1), 61–68. https://doi.org/10.1038/s41561-018-0251-0.

Stephenson, S.N., Hoggard, M.J., Holdt, M.C., White, N., 2024. Continental residual topography extracted from global analysis of crustal structure. Journal of Geophysical Research: Solid. Earth 129. https://doi.org/10.1029/2023JB026735 e2023JB026735.

Stern, R.J., 1994. Arc assembly and continental collision in the Neoproterozoic East African orogen. Annu. Rev. Earth Planet. Sci. 22, 319–351.

Stern, R.J., 2002. Crustal evolution in the East African Orogen: a neodymium isotopic perspective. J. Afr. Earth Sci. 34 (3–4), 109–117.

Stow, D., Nicholson, U., Kearsey, S., Tatum, D., Gardiner, A., Ghabra, A., Jaweesh, M., 2020. The Pliocene-recent Euphrates river system: Sediment facies and architecture as an analogue for subsurface reservoirs. Energy Geosci. 1 (3–4), 174–193.

Straume, E.O., Steinberger, B., Becker, T.W., Faccenna, C., 2024. Impact of mantle convection and dynamic topography on the Cenozoic paleogeography of Central Eurasia and the West Siberian Seaway. Earth Planet. Sci. Lett. 630, 118615.

Stüwe, K., Robl, J., Matthai, S., 2009. Erosional decay of the Yucca Mountain crest. Nevada. Geomorphology 108 (3–4), 200–208.

Stüwe, K., Robl, J., Turab, S.A., Sternai, P., Stuart, F.M., 2022. Feedbacks between sea-floor spreading, trade winds and precipitation in the Southern Red Sea. Nat. Commun. 13 (1), 5405.

Styron, R., Pagani, M., 2020. The GEM global active faults database. Earthq. Spectra 36 (1_suppl), 160–180.

Tang, Z., Mai, P.M., Chang, S.J., Zahran, H., 2018. Evidence for crustal low shear-wave speed in Western Saudi Arabia from multi-scale fundamental-mode Rayleigh-wave group-velocity tomography. Earth Plan. Sci. Lett. 495, 24–37. https://doi.org/10.1016/j.epsl.2018.05.011.

Telbisz, T., Kovács, G., Székely, B., Szabó, J., 2013. Topographic swath profile analysis: a generalization and sensitivity evaluation of a digital terrain analysis tool. Z. Geomorphol. 57 (4), 485–513.

Thiede, R.C., Bookhagen, B., Arrowsmith, J.R., Sobel, E.R., Strecker, M.R., 2004. Climatic control on rapid exhumation along the Southern Himalayan Front. Earth Plan. Sci. Lett. 222 (3–4), 791–806.

Thrastarson, S., van Herwaarden, D.P., Noe, S., Josef Schiller, C., Fichtner, A., 2024. REVEAL: a global full-waveform inversion model. Bull. Seism. Soc. Am. 114 (3), 1392–1406.

Tiberi, C., Ebinger, C., Ballu, V., Stuart, G., Oluma, B., 2005. Inverse models of gravity data from the Red Sea-Aden-East African rifts triple junction zone. Geophys. J. Int. 163, 775–787. https://doi.org/10.1111/j.1365-246X.2005.02736.x.

Trifonov, V.G., Dodonov, A.E., Sharkov, E.V., Golovin, D.I., Chernyshev, I.V., Lebedev, V. A., Ali, O., et al., 2011. New data on the late Cenozoic basaltic volcanism in Syria, applied to its origin. J. Volc. Geotherm. Res. 199 (3–4), 177–192.

Tsekhmistrenko, M., Sigloch, K., Hosseini, K., Barruol, G., 2021. A tree of Indo-African mantle plumes imaged by seismic tomography. Nat. Geosci. 14 (8), 612–619. https://doi.org/10.1038/s41561-021-00762-9.

Turab, S.A., Stüwe, K., Stuart, F.M., Cogne, N., Chew, D.M., Robl, J., 2023. A two phase escarpment evolution of the Red Sea margin of southwestern Saudi Arabia. Insights from low-temperature apatite thermochronology. Earth Plan. Sci. Lett. 603, 117990.

Turcotte, D.L., Schubert, G., 1982. Geodynamics: Applications of Continuum Physics to Geological Problems. John Wiley, New York.

Ukstins Peate, I., Bryan, S.E., 2008. Re-evaluating plume-induced uplift in the Emeishan large igneous province. Nat. Geosci. 1 (9), 625–629.

Vigny, C., Huchon, P., Ruegg, J.C., Khanbari, K., Asfaw, L.M., 2006. Confirmation of Arabia plate slow motion by new GPS data in Yemen. J. Geophys. Res.-Sol. Ea. 111 (B2).

Viltres, R., Jónsson, S., Alothman, A.O., Liu, S., Leroy, S., Masson, F., et al., 2022. Present-day motion of the Arabian plate. Tectonics 41 (3) e2021TC007013.

Wegmann, K.W., Pazzaglia, F.J., 2009. Late Quaternary fluvial terraces of the Romagna and Marche Apennines, Italy: Climatic, lithologic, and tectonic controls on terrace genesis in an active orogen. Quat. Sci. Rev. 28 (1–2), 137–165.

Wegmann, K.W., Zurek, B.D., Regalla, C.A., Bilardello, D., Wollenberg, J.L., Kopczynski, S.E., Pazzaglia, F.J., et al., 2007. Position of the Snake River watershed divide as an indicator of geodynamic processes in the greater Yellowstone region, western North America. Geosphere 3 (4), 272–281.

Wei, W., Zhao, D., Wei, F., Bai, X., Xu, J., 2019. Mantle dynamics of the eastern Mediterranean and Middle East: Constraints from P-wave anisotropic tomography. Geochem. Geophys. Geosy. 20 (10), 4505–4530. https://doi.org/10.1029/2019gc008512.

Weissbrod, T., Gvirtzman, G., 1989. Crustal thinning possibly related to late paleozoic updoming: evidence from two near eastern megastructures. Bulletin de la Société belge de géologie 98 (2), 235–237.

Weissel, J., Malinverno, A., Harding, D., 1995. Erosional development of the Ethiopian Plateau of Northeast Africa from fractal analysis of topography. In: Barton, C.C., Pointe, P.R. (Eds.), Fractals in Petroleum Geology and Earth Processes. Plenum Press, New York, pp. 127–142.

Wessel, P., Luis, J.F., Uieda, L.A., Scharroo, R., Wobbe, F., Smith, W.H., Tian, D., 2019. The Generic Mapping Tools version 6. Geochem. Geophys. Geosyst. 20, 5556–5564.

Williams, M., 2019. The sudd swamps and the white nile. The Nile Basin: Quaternary Geology, Geomorphology and Prehistoric Environments. Cambridge University Press, Cambridge, p. 107e126. https://doi.org/10.1017/9781316831885.009.

Wolfenden, E., Ebinger, C., Yirgu, G., Renne, P.R., Kelley, S.P., 2005. Evolution of a volcanic rifted margin: Southern Red Sea, Ethiopia. Geol. Soc. Am. Bull. 117 (7–8), 846–864.

Yao, Z., Mooney, W.D., Zahran, H.M., Youssef, S.E.H., 2017. Upper mantle velocity structure beneath the Arabian shield from Rayleigh surface wave tomography and its implications. J. Geophys. Res.-Sol. Ea. 122 (8), 6552–6568. https://doi.org/10.1002/2016JB013805.

Yeats, R., 2012. Active Faults of the World. Cambridge University Press.

Ziegler, M.A., 2001. Late Permian to Holocene paleofacies evolution of the Arabian plate and its hydrocarbon implications. GeoArabia 6, 445–504.

Zilberman, E., 1991. Landscape evolution in the central, northern and northwestern Negev during the Neogene and the Quaternary. Isr. Geol. Surv. Rep. GSI/45/90, 164 pp.

Zilberman, E., Calvo, R., 2013. Remnants of Miocene fluvial sediments in the Negev Desert, Israel, and the Jordanian Plateau, evidence for an extensive subsiding basin in the northwestern margins of the Arabian plate. J. Afr. Earth Sci. 82, 33–53.